

# **Short-term Prediction of Regional Wind Power Production**

**Lars Landberg, Risø National Laboratory (DK)**

**Hans-Peter Waldl, University of Oldenburg (DE)**

Gregor Giebel, Risø National Laboratory (DK)

Ulrich Focken, Matthias Lange, Kai Mönnich, University of Oldenburg (DE)

Hans Georg Beyer, Armin Luig, Technical College of Magdeburg (DE)

Contract JOR3-CT97-0272 PL971254

## **Publishable Final Report**

July 1998 to December 1999

Research funded in part by  
**THE EUROPEAN COMMISSION**  
in the framework of the  
Non Nuclear Energy Programme  
**JOULE III**





# Contents

<b>1</b>	<b>Abstract</b>	<i>1</i>
<b>2</b>	<b>Partnership</b>	<i>2</i>
<b>3</b>	<b>Objectives</b>	<i>3</i>
<b>4</b>	<b>Technical Discription</b>	<i>4</i>
4.1	Overview	<i>4</i>
4.2	Numerical Weather Prediction Models	<i>5</i>
4.3	The Oldenburg Prediction Model	<i>5</i>
4.4	The Risø Model	<i>8</i>
4.5	Differences between Oldenburg and Risø Implementation	<i>18</i>
<b>5</b>	<b>Results and Conclusions</b>	<i>19</i>
5.1	Wind Speed	<i>19</i>
5.2	Power Prediction Time Series	<i>20</i>
5.3	Prediction Horizon and Daily Pattern	<i>23</i>
5.4	Online Data 1999	<i>28</i>
5.5	Prediction Error and Mean Power Output	<i>29</i>
5.6	MOS	<i>31</i>
5.7	HIRLAM/Deutschlandmodell	<i>34</i>
5.8	Power output of spatially distributed Turbines	<i>35</i>
5.9	Ensemble Smoothing of Forecast Errors	<i>36</i>
5.10	Different Regions	<i>37</i>
5.11	Conclusions	<i>39</i>
<b>6</b>	<b>Exploitation</b>	<i>41</i>
<b>7</b>	<b>Characteristic Diagram</b>	<i>43</i>
<b>A</b>	<b>References</b>	<i>44</i>
<b>B</b>	<b>List of publications</b>	<i>45</i>

# Nomenclature

DM	<i>Deutschlandmodell</i> , the German NWP
DWD	<i>Deutscher Wetterdienst</i> , the German weather service
DMI	<i>Danish Meteorological Institute</i>
DEWI	The German Wind Energy Institute
EURE	European Utilities for Renewables
FLaP	The Univ of Oldenburg wind farm program
HIRLAM	The Danish NWP
NWP	Numerical weather prediction model
PARK	The Risø wind farm program
FLaP	The Oldenburg wind farm program
WMEP	A German wind and wind power measuring project
WASP	Wind Atlas Analysis and Application Program
Short term	Here: concerning a time range from 3 to 48 hours



# 1 Abstract

The main objective of this project was to implement a wind power forecasting system for a time period up to 48 hours, extending an approach developed in other EU and national projects.

This forecasting approach developed in the framework of this project gives the project partners the possibility to implement this method for utilities, tailored to the respective situation concerning installed power, topographical conditions, and so on.

In practice, the forecasting system can be one basis for a better scheduling of conventional power plants leading to a lower spinning reserve and thereby to savings of fossil fuel and CO<sub>2</sub>. Besides this, a better integration of wind energy in the existing electric energy supply systems leads to a better acceptance of this new technology.

During the project time a fully operationally working wind power prediction system has been developed. With this system it is possible to predict the power output for single turbines, wind farms or larger regions up to 48 hours ahead.

The performance of the prediction system was investigated by means of statistical analysis comparing forecasts to wind turbine power output measurements from about 30 sites. Main result of this part is that the is almost independent of wind speed and kind of an absolute measure, which is typically in the range of 15 % (6 hours prediction) to 25 % (48 hours) of rated power.

Looking at the summed up power output from regions, the prediction error decreased due to smoothing effects. A typical reduction of RMSE is to 60 % to 80 % of the single farm value, concerning a region of about  $100 \times 200 \text{ km}^2$ .

## 2 Partnership

The partnership consists of three partner institutions:

- Risø National Laboratory, Denmark: model development, model implementation, model verification, co-ordination.
- University of Oldenburg, Germany: model development, model implementation, model verification, study of regional effects.
- Technical College of Magdeburg, Germany: study of regional effects.

Addresses of partners:

**Risø National Laboratory** (Coordinator)  
Dept Wind Energy and Atmospheric Physics  
PO Box 49  
DK-4000 Roskilde  
DENMARK  
*Contact:*  
Lars Landberg  
email lars.landberg@risoe.dk  
fon +45 46 77 50 24  
fax +45 46 77 59 70

**University of Oldenburg**  
Energy- and Semiconductor Research  
Faculty of Physics  
D-26111 Oldenburg, Germany  
*Contact:*  
Hans-Peter Waldl  
email igor@uni-oldenburg.de  
fon +49 441 798 3577  
fax +49 441 798 3326

**Technical College of Magdeburg**  
Dept. of Electrical Engineering  
D-39114 Magdeburg, Germany  
*Contact:*  
Prof. Dr. Hans Georg Beyer  
email Hans-Georg.Beyer@Elektrotechnik.FH-Magdeburg.de  
fon +49 391 8864499  
fax +49 391 8864126

The project WWW page:

[www.physik.uni-oldenburg.de/ehf/wind/predict/indexpredict.html](http://www.physik.uni-oldenburg.de/ehf/wind/predict/indexpredict.html)

### 3 Objectives

The main objective of this project was to implement a wind power forecasting system for a time period up to 48 hours, extending an approach developed in other EU and national projects. This forecasting approach developed in the framework of this project gives the project partners the possibility to implement this method for utilities, tailored to the respective situation concerning installed power, topographical conditions, and so on.

In practice, the forecasting system can be one basis for a better scheduling of conventional power plants leading to a lower spinning reserve and thereby to savings of fossil fuel and CO<sub>2</sub>. Besides this, a better integration of wind energy in the existing electric energy supply systems leads to a better acceptance of this new technology.

In the near future, the trading with “green energy” will become an essential part of energy markets. The resulting price of green electric energy will depend on the day by day availability of this energy source. So not only “classic” energy suppliers but also “green traders” are becoming potential customers for wind power forecasts.

The **main technical objectives** of the project have been

- **Implementing a prediction method on base of the German NWP model.** Due to the coarse resolution of the *Deutschlandmodell* model ( $14 \times 14 \text{ km}^2$ ), a spatial refinement of the prediction must be implemented to get a forecast tailored to a specific site.
- **Make an analysis of the prediction error for the mean power output for an area considered.** The described method delivers wind power predictions for different sites. The regional power production is then derived by multiplying this result with a factor. For power plant dispatching, utilities are not only interested in power output for single wind farms but also for their total supply area. The quality of prediction and especially its uncertainty may be different for one point analysis and the whole area. In this project, an estimation of the prediction error in dependence on the size of the area under investigation was developed on base of a comparison of predicted and measured wind power for about 30 sites distributed over Northern Germany.
- **Using a numerical weather prediction model with a higher spatial and temporal resolution than in former projects as base for the power prediction model.** As numerical weather prediction model (NWP), the German *Deutschlandmodell* was chosen. The goal is to investigate whether or not the higher resolution results in a better prediction of wind speed and wind power output compared to HIRLAM.

# 4 Technical Discription

## 4.1 Overview

During the project time a fully operationally working prediction system has been developed. With this system it is possible to predict the power output for single turbines, wind farms or larger regions. It delivers the respective power output as well as wind speed and direction in an easily readable output format. Input for the system can be online or archive wind speed and wind direction predictions from an overall numerical weather forecast. The prediction system may be operated by the german weather forecast DWD, when wind energy power forecasts are requested by energy suppliers or (green) energy brokers. The project consisted of the following parts all of which will be described in the following:

- Model development
- Model implementation
- Model evaluation
- Study of regional effects

### Model development

A model was developed further which produces wind power predictions taking into account the local circumstances like surface roughness and orography. The forecasts are based on the output of numerical weather prediction models, the Danish HIRLAM and the German *Deutschlandmodell*.

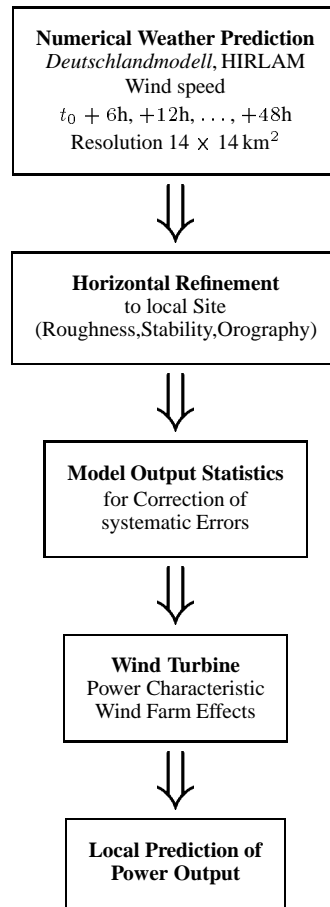
### Model implementation

The prediction model was implemented as an online prediction system getting weather prediction data from the according weather service, and generating the locally refined wind power forecasts (see overview next page). As an user interface, HTML pages are generated.

### Model evaluation

For assessment of the quality of the predictions, measuring data from 32 stations spread over the northern part of Germany for three years was used. An intensive comparison of measurements and predictions was performed. One focus was the statistical analysis of smoothing effects occuring if the regional power output from regions is investigated.

In the following, the forecast models developed and used in the project will be described. The two models used are called the Risø model and the Oldenburg model. Both these models use numerical weather prediction (NWP) model forecasts as the basis for the more detailed local forecasts. In this project the HIRLAM model of the Danish Meteorological Institute was used as the NWP model for the Risø model and the *Deutschlandmodell* (DM) for the Oldenburg model. In the following HIRLAM and DM are described followed by a detailed description of the Risø and Oldenburg models.



*Overview of the different parts of the prediction systems.*

## 4.2 Numerical Weather Prediction Models

As basic input to the prediction systems, two different numerical weather prediction models (NWP) were used: the Danish HIRLAM model and the German *Deutschlandmodell*. They are operated by the respective weather services.

	<b>HIRLAM</b>	<b>Deutschlandmodell DM</b>
Operator	Danish Meteor. Institute	German Weather Service
Horiz. Grid Resolution	25 km	15 km
Starting Times	0 and 12 GMT	0 and 12 GMT
Domain	Denmark and Northern Germany	Germany and Neighborhood

*Main properties of the two NWP models.*

## 4.3 The Oldenburg Prediction Model

As the Risø model, the Oldenburg approach is based on the predictions of a numerical weather prediction model, the *Deutschlandmodell* operated by the *German Weather Service* ([16]). The results of this model have a resolution of  $14 \times 14 \text{ km}^2$ . Several steps are undertaken to get a local prediction taking into account the specific local conditions on a site (figure 1). This mechanism transforms the NWP result (height 10 m or a model level) to the hub height of the according turbine. This includes the consideration of local roughness, obstacles, orography, thermal stratification of the atmosphere, wind turbine parameters and wind farm arrangement. In addition, a correction of systematic errors is done with a simple statistical model.

The transformation of the surface wind is done on base of methods following the *European Wind Atlas Method*. To get a closer look on the influence of model details on the prediction uncertainty, the models described below were implemented new.

#### 4.3.1 Spatial Refinement: Roughness

To generalize the NWP wind output from the used roughness, in a first step the geostrophic wind is calculated from the 10 m value using the geostrophic drag law

$$G = \frac{u_*}{\kappa} \sqrt{\left(\ln\left(\frac{u_*}{f z_0}\right) - A(\mu)\right)^2 + B(\mu)^2} \quad (1)$$

by using  $u_*$  and  $z_0$  of the *Deutschlandmodell* wind ( $f$ : Coriolis parameter,  $A, B$ : constants, in general depending on stability factor  $\mu$ ). Backward, the local wind then is calculated by using the local, sectorial differentiated roughness length and the current atmospheric stability ([13],[7]).

$$u(z) = \frac{u_*}{\kappa} \left( \ln\left(\frac{z}{z_0}\right) - \Psi\left(\frac{z}{L}\right) \right) \quad (2)$$

The turning of the wind in the Ekman layer is modelled with the standard approach

$$\sin \alpha = -\frac{B(\mu) u_*}{\kappa G} \quad (3)$$

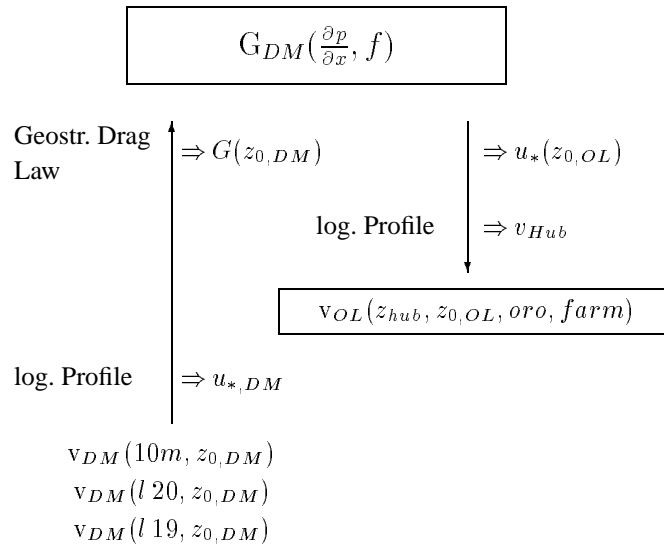


Figure 1: Transformation of surface wind speed to the geostrophic wind and back with the detailed roughness description.

For higher model levels (here level 18 and higher), the left branch of figure 1 is omitted and the level wind is used just as geostrophic wind directly.

In the surrounding of a site, in general the roughness is inhomogeneous. Different roughness lengths result in different vertical wind speed profiles. In the right branch of figure 1, the calculations are made including a detailed roughness description depending on wind direction and distance to the site. An algorithm was implemented which takes into account the development of internal boundary layers ([14]).

### 4.3.2 Spatial Refinement: Stability

The vertical wind speed profile depends on the thermal stratification of the atmosphere (see equation 2;  $L$ , the Monin-Obhukov length, is a measure for the thermal stratification, see [13]). To take into account this stratification, the information about the (predicted) thermal state of the atmosphere must be obtained together with the wind speed predictions. Because the German Weather Service does not provide this value online, we used the longterm climatological mean value of  $L$  to make an overall correction to all prediction. Of course, this cannot be satisfactory, because meteorological effects like the daily pattern of wind speed depend strongly on  $L$ . Fortunately, at higher wind speeds which are important for wind energy use, the atmosphere in most cases is nearly neutral, so the influence of the missing online inclusion of the stratification should not be too high.

The consideration of the stratification is done according to the European Wind Atlas method. The vertical wind speed profile is regarded as being disturbed by non neutral conditions by implying a function  $f(z)$ :

$$u(z) = u_0(z) \left( 1 + \frac{\Delta u(z_m)}{z_0(z_m)} f(z) \right) \quad (4)$$

The term  $\frac{\Delta u(z_m)}{z_0(z_m)}$  is derived with

$$\frac{\Delta u(z_m)}{u_0(z_m)} = \frac{\Delta u_*}{u_*0} - \frac{\psi(z_m/L_{off}) + \psi(z_m/L_{rms})}{\ln(z_m/z_0)} \quad (5)$$

. Regarding the climatological mean for Central Europe, following values were chosen: heat flows  $\Delta H_{off} = 100 \text{ W/m}^2$  (multiplied with a form factor of  $F=0.6$ ) and  $\Delta H_{rms} = -40 \text{ W/m}^2$ .

The according Monin-Obukhov-length is defined via

$$L = \frac{T_0 c_p u_*^3 \rho}{\kappa g H_0} \quad (6)$$

The height  $z_m$  depends on roughness length  $z_0$  and Rossby number  $Ro = G/f z_0$  and so connects the roughness and the stability model.

$$z_m = 0.002 z_0 Ro^{0.9} \quad (7)$$

The ratio  $\frac{\Delta u_*}{u_*}$  can be derived from the total differential of the geostrophic drag law

$$\frac{du_*}{u_*} = \left[ \frac{c g}{f T_0 c_p \rho G^2} \right] dH \quad (8)$$

The constant has the value  $c = 2.5$ .

The function  $f(z)$  is responsible for the shape of the vertical profile

$$f(z) = 1 - \frac{\ln(z_m/z_0)}{\ln(z/z_0)}. \quad (9)$$

### 4.3.3 Complex Terrain

In complex terrain, the wind speed is changed in amount and direction by orographic effects. These effects are taken into account by using the calculation results from WASP. These are given as an MTX file including a correction factor for wind speed and wind direction for each direction sector. WASP itself implements a linear model of ‘‘Jackson-Hunt’’ type ([15]). Base of the model calculations is a digital orographic map of the surrounding of the turbine site. First, the wind speed is turned by the value given by the WASP results. Then, the speed up factor is multiplied to the wind speed.

#### 4.3.4 Wind Farm Effects

Inside a wind farm, the mutual influence of the turbines to each other result in a reduction of power output. This reduction is depending on the geometrical arrangement of the turbines, the wind direction and on wind speed. The farm effects are calculated by the Oldenburg computer programs called `FLaP` resp. `fcalc`, which implement a variant of the so called *Risø-Model* like used for instance in the Risø program `Park` ([17]).

Each farm is characterised by its arrangement, turbine power and thrust coefficient characteristics. For the given wind farm (or a single turbine inside a farm) a table of reduction factors is calculated depending on wind direction and wind speed. This factor is multiplied to the farm or turbine output at the end of the prediction model.

### 4.4 The Risø Model

In this section the physical model of Risø National Laboratory is described. Each step, from selecting the HIRLAM wind to the final MOS corrections, will be described in turn. An overview of the model is given in Figure 2. The analysis of the original model will show, that when focus is on severe storms the model can be improved in some ways. Furthermore, a re-analysis of the winds from the various levels of HIRLAM will show that better predictions can be made using a different level. The final model will be described at the end of this section.

#### 4.4.1 Overview

The forecasting system from the output from HIRLAM to the final forecast at the utility is sketched in Figure 2.

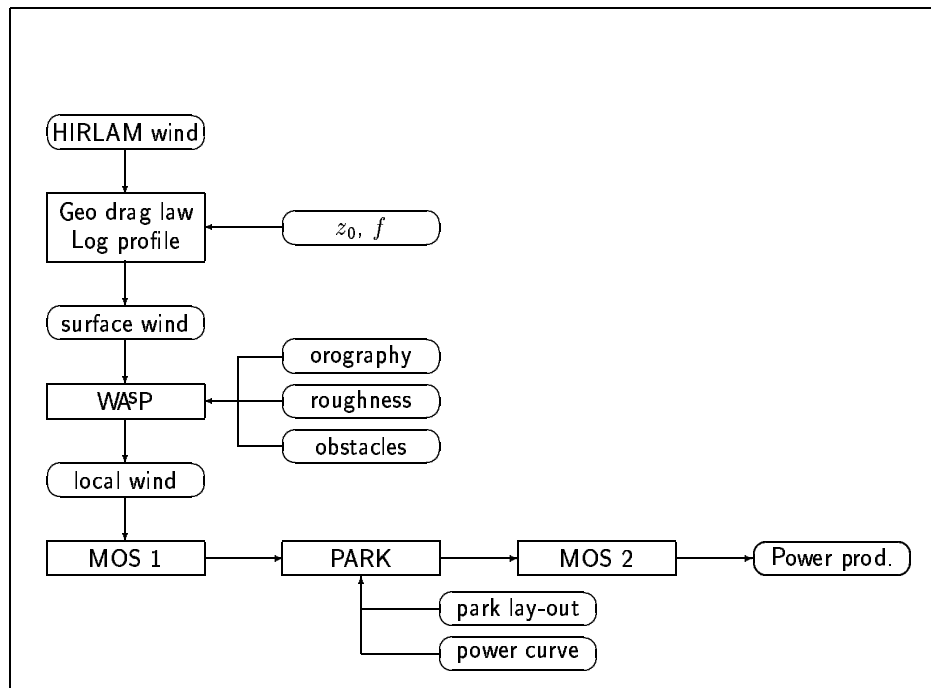


Figure 2: Flow chart of the model complex from the HIRLAM wind to the final prediction of the power output from a wind farm.

#### 4.4.2 HIRLAM

The large-scale flow of the atmosphere is modeled by the E-version of HIRLAM of the Danish Meteorological Institute. The model has a horizontal resolution of 16 km and it is run four times a day at 00, 06, 12 and 18 UTC.

**Finding the right HIRLAM level** Since HIRLAM has a vertical grid of 31 levels it is necessary to investigate which level gives the wind that best approximates the geostrophic wind (a theoretical wind). To do this an analysis has been carried out on a subset of the wind farms, where the model has been run with HIRLAM winds from level 1 (65 m) to level 7 (1050 m). The results are shown in Figures 3 and 4.

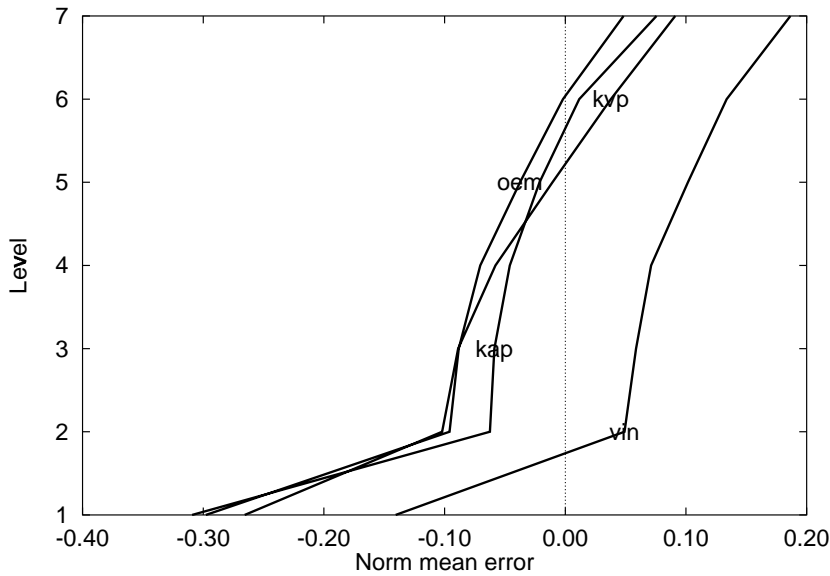


Figure 3: The mean of the error for the 12 hour prediction normalised with the total capacity of the wind farm as a function of the level.

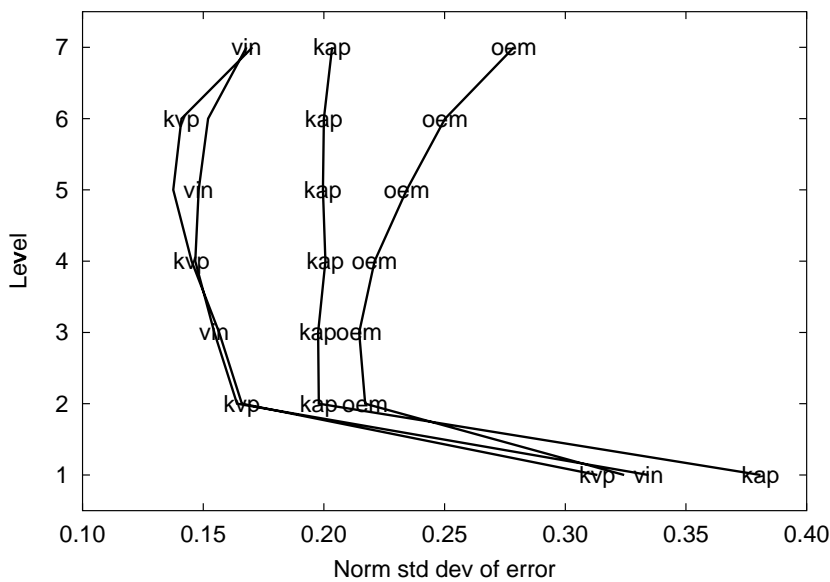


Figure 4: The standard deviation of the error for the 12 hour prediction normalised with the total capacity of the wind farm as a function of the level.

Analysing these two plots, a number of observations can be done:

- Vindeby seems to be very different from the others, we will return to this in a later section. Here, we will not put emphasis on this station when drawing our conclusions.
- The mean error is closest to zero at levels 5 and 6.
- The std. dev. of the error is smallest again for levels 5 and 6

These observations lead to a choice between either level 5 or level 6. Level 5 have been chosen, because it has the overall smallest error and most stations have the smallest or second smallest std. dev. of the error. In the following, therefore, *the geostrophic wind,  $G$ , will be set equal to the wind obtained from level 5 (ie at 550 m agl) of HIRLAM*. Note, that it is the *actual* HIRLAM wind which is used, not the geostrophic HIRLAM wind. It was found that this wind gave too high standard deviations of the error. This is in agreement with the findings in Landberg et al, 1993.

#### 4.4.3 Surface transformation

The idea behind the physical model is that the predicted wind from HIRLAM, which is a wind specific to a gridcell of  $23 \times 23 \text{ km}^2$ , is transformed to the surface using the geostrophic drag law (cf Blackadar and Tennekes, 1968),

$$G = \frac{u_*}{\kappa} \sqrt{\left[ \ln \left( \frac{u_*}{f z_0} \right) - A \right]^2 + B^2} \quad (10)$$

where  $G$  is the geostrophic wind, here set equal to the HIRLAM wind at level 5,  $u_*$  the friction velocity,  $\kappa$  the Von Kármán constant ( $=0.4$ ),  $f$  the Coriolis parameter, and  $z_0$  the aerodynamic roughness length.  $A$  and  $B$  are constants here set equal to 1.8 and 4.5, respectively, in accordance with Troen and Petersen (1989).

The geostrophic drag law gives the friction velocity which can be used to get a velocity in the surface boundary layer by using the logarithmic wind profile

$$u(z) = \frac{u_*}{\kappa} \ln \left( \frac{z}{z_0} \right) \quad (11)$$

where  $u(z)$  is the velocity at height  $z$ . These equations are in their neutral form. For further details, see Landberg and Watson (1994).

#### 4.4.4 WASP

The wind calculated so far is still valid for quite a big area and it must be corrected to take local effects into account. This is done using WASP (Wind Atlas Analysis and Application Program, Mortensen et al, 2000). WASP is taking the following local effects into account:

- Shelter from obstacles (houses, wind breaks etc).
- Effects of roughness and changes in roughness.
- Effects of the orography, speed-up/down.

Note, that this list does not include thermally-driven effects as e.g. sea-breezes and katabatic winds. In most of Northern Europe (including Denmark) these latter effects will not be of any importance, and can thus be left out without any loss of accuracy. The problem of thermally-driven effects must be addressed, however, if the model is to be used in areas where those effects prevail (eg the Mediterranean).

From the previous study (Landberg and Watson, 1994 and Landberg et al, 1993) an estimate of the RMS error gave around  $1.5 \text{ ms}^{-1}$  for a typical station in Northern Europe. The

study also showed that implementing MOS (Model Output Statistics) greatly improved the predictions for some of the stations, and as a consequence this method will also be used in this study to explain the effects not explained by the physical models.

The parameters in the MOS model will be estimated using detailed measurements from the 17 wind farms and model output from HIRLAM. The measurements consist of data from the individual turbines plus a number of meteorological parameters at each farm taken at one-hourly intervals.

A further refinement of the method could be to include time dependent roughness descriptions, this is due to the fact that roughness is actually a time-varying quantity (eg trees have leaves in the the summer and none during winter), the only one in the list above. The time-variance of roughness is not taken into account in WAsP because WAsP is estimating climatological quantities (eg the yearly production), and therefore it would be wrong to let the roughness vary; in the present approach, on the other hand, we look at individual times, making it necessary to examine the inclusion of this time dependence. The time variability of the roughness could be included by making four different roughness descriptions: one for each season.

#### 4.4.5 Model Output Statistics (MOS)

To correct for all effects not explained by the models, Model Output Statistics (MOS) is used. A number of different approaches can be taken.

Firstly, the functional form of the MOS filter must be chosen. Studying the behaviour of the error (cf Figure 5) it can be seen that the only reasonable candidate is the simple linear function:

$$y(\text{final, sector}) = y(\text{model, sector})a(\text{sector}) + b(\text{sector}) \quad (12)$$

where  $y(\text{final, sector})$  is the final forecast,  $y(\text{model, sector})$  the forecast from the physical models,  $a(\text{sector})$  and  $b(\text{sector})$  are the direction dependent constants of the linear function.

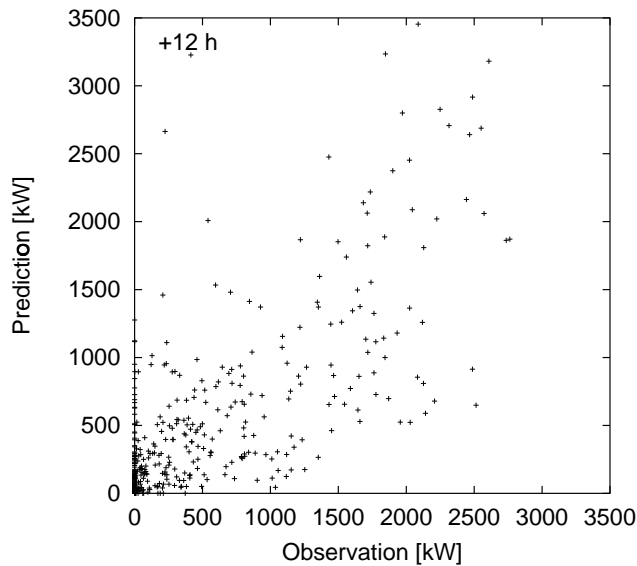


Figure 5: Scatter plot of the raw physical prediction vs the observation for the Kyndby wind farm for the 12 hour prediction length.

The second choice concerns the point at which the MOS filter is to be applied. Here a number of possibilities present themselves:

1. the output could be corrected right after the local wind has been calculated (and before the application of the power curve and the park effects).
2. to correct after the power has been calculated
3. to correct the end product of the model.

It has also to be decided whether MOS should be applied to the predictions as a whole or whether it should be applied to the predictions sector by sector. All these possibilities have been looked into and the findings are described in the following.

Before any MOS is applied it is necessary to determine whether any of the input to the physical models can be improved: is there eg a station which is consistently under-predicted, and is this station located in a flat area, then it is more than likely that the roughness assigned to the area is too high. It was found that if corrections are applied sector by sector (see later) they did not consistently stay under/over 1.0 for any one station. This means that the roughnesses most likely has been assigned the correct values. It could, however, also just mean that the signal for the effect of roughness is overwritten by signals from other error sources. It is therefore decided not to change the roughness for any of the stations.

Another reason for not changing the roughness lengths is that the values used are the standard values for the Danish landscape (cf Table 1).

*Table 1. Standard roughness lengths,  $z_0$ , for typical Danish landscapes.*

Type	$z_0$ [m]
Sea	$10^{-4}$
Village	0.35
City	0.4-0.5
Forrest	0.35-0.4
Farmland	0.1

**MOS applied to the wind speed** There can be no doubt that the best place to apply MOS is as early as possible, namely, at the predicted local wind.

One could also apply MOS to the geostrophic wind itself, but this would make the statistical corrections the dominating part, and overshadow the abilities of the physical models to explain the local variation of the wind. This latter approach would therefore be more like a statistical approach, than a physical one. Since we have set out to use the available physical models as far as possible, correcting the geostrophic wind will not be done.

The observed wind is unfortunately measured *on* the nacelle of the wind turbines, causing severe flow distortion. On top of this the anemometers were never meant as precision devices for measuring the wind, so it has been decided not to use the speed measurements. Another very unfortunate thing is the fact that wind direction is not measured at all. We know, however, from a previous study (Landberg and Watson, 1994) that the direction is predicted fairly well. All this leads to the conclusion that MOS should not be applied directly to the wind speed.

**MOS applied to the power** Taking the above findings into account, it is found that MOS must be applied to the power prediction. Since the power curve distorts the wind speeds quite significantly, leaving small variations in wind speed very important in some places and completely unimportant in others, the following procedure has been devised. It assumed that the real wind speed (of which we have no reliable measurement),  $\hat{u}$ , is connected to the predicted wind speed by the following simple relation:

$$\hat{u} = a_i u_{\text{pred}} \quad (13)$$

where  $a_i$  is the factor for the  $i$ 'th sector and  $u_{\text{pred}}$  is the predicted wind speed. Folding this back through the power curve, we get:

$$P_{\text{obs}} \simeq P_{\text{pred}} = p(a_i u_{\text{pred}}) \times T \times E \quad (14)$$

where  $P_{\text{obs}}$  and  $P_{\text{pred}}$  are the observed and predicted power, respectively, of a given wind farm,  $p(u)$  is the power a given turbine will produce at speed  $u$  (ie the power curve),  $T$  is the number of turbines operating, and  $E$  the efficiency of the wind farm as calculated by PARK.

It is then possible to find that  $a$  which for a certain sector gives the smallest value of the error:

$$e = |P_{\text{obs}} - P_{\text{pred}}| \quad (15)$$

The functional shape of  $e$  as a function of  $a$  can be seen in Figure 6. It can be seen that the function is well behaved, which means that simple methods for minimising  $e$  can be used.

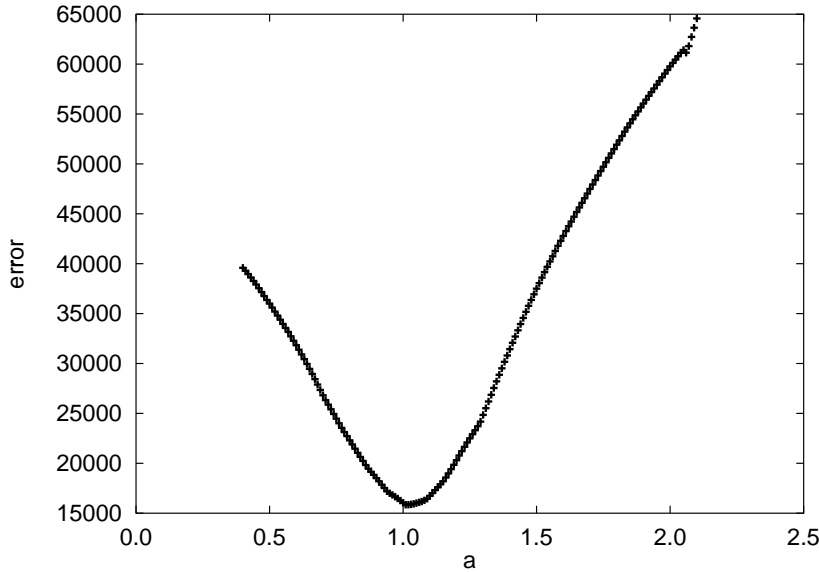


Figure 6: Typical example of the error,  $e$ , plotted as a function of the MOS parameter  $a$ .

**Estimating the final  $a$ 's** Following the above procedure a value for  $a$  can be calculated for each sector and for each forecast length. Doing this, a typical example of the calculated values is found in Figure 7. As can be seen from this figure, most of the calculated  $a$ 's do not vary with the forecast length. This is also to be expected, since it is hypothesised that the effects, that the  $a$ 's correct for, are *physical* effects, which are independent of the forecast length. Some sectors, however, display quite a large variation (in the figure, sectors 1, 2 and 11), this is explained by the fact that the number of samples in these sectors is down to only 25% of the average number of samples for all sectors, and these sectors are thus not statistically stable.

To calculate one  $a$  per sector (ie to collapse the  $a$ 's in the forecast length direction) the average of the  $a$ 's for the different prediction horizons is used.

A final question pertaining to the sector-wise corrections is the constancy with time of the estimates, ie for how long must one wait until the factors have stabilised. A typical

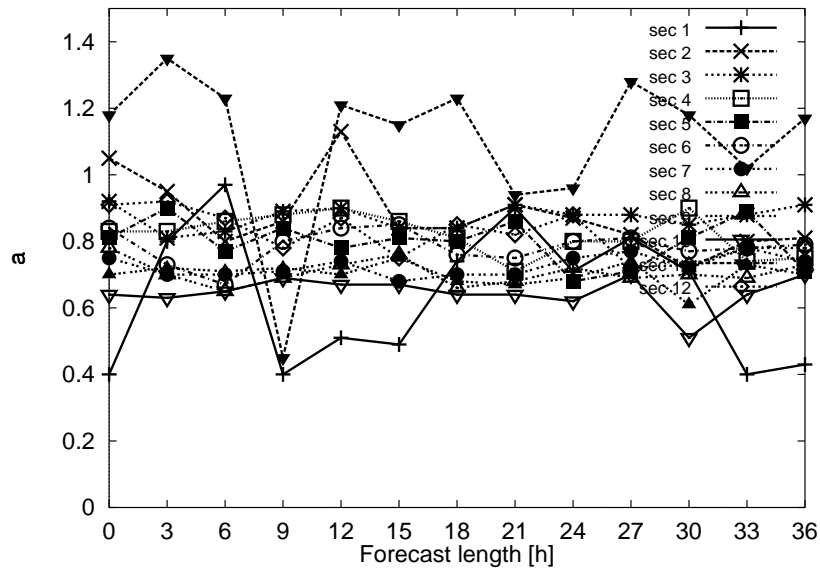


Figure 7: The MOS-correction factor for each of the twelve 30 degree sectors for the different prognosis lengths.

example of this is given in Figure 8. Studying this figure it can be seen that most factors are stable after only a few months, except of course seldomly visited sectors (1, 2 and 12 in the figure). Sector 3 stands out in that the total amount of observations over the year is large enough, but during the first few months very few observations are present, explaining the marked swing after two months. The pattern found for this wind farm is repeated for the other wind farms as well.

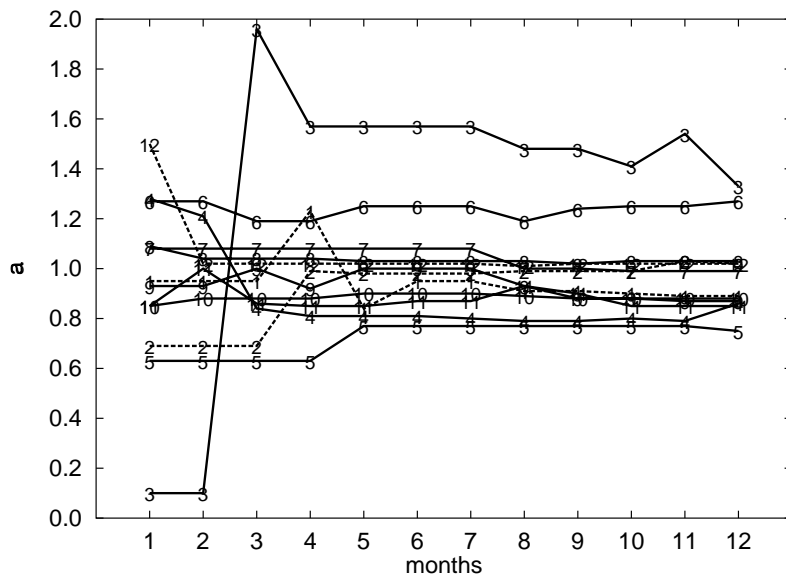


Figure 8: The variation with time of the estimate of the sector-wise MOS correction factor. Sectors with very few observations are marked with dashed lines. The data are taken from the Nøjsomhedsodde Wind Farm.

**MOS applied to the final output** To correct for any *bias* another simple MOS model has been chosen to correct the *final* output of the model, ie the actual production of the park. A simple linear version of MOS is again used

$$P_{\text{MOS}} = P_{\text{model}} + b \quad (16)$$

where  $P_{\text{MOS}}$  is the MOS-corrected production of a given wind farm (ie the final result of the model),  $P_{\text{model}}$  the production predicted by the physical model, and  $b$  the bias. Note that  $b$  is not dependent on the sector, since it is assumed that the first MOS module took care of any directional differences.

#### 4.4.6 PARK

To take into account the influence of wakes hitting other turbines in the park the PARK program (Sanderhoff, 1993) has been used to create a park efficiency rose (ie a sector-wise list of the actual production seen relative to the rated production).

#### 4.4.7 Input to the model

To be able to predict the power output of a wind farm the following input is needed:

- HIRLAM wind field (Geo. drag law)
- description of orography (WASP)
- description of roughness (WASP)
- description of obstacles (WASP)
- power curve (PARK)
- thrust curve (PARK)
- wind farm lay-out (PARK)
- measurements of actual power production (MOS)

Note that this information, except for the HIRLAM forecast, is needed only for the initial analysis of the wind farm, once the farm is analysed the prediction model uses only the results of the analysis.

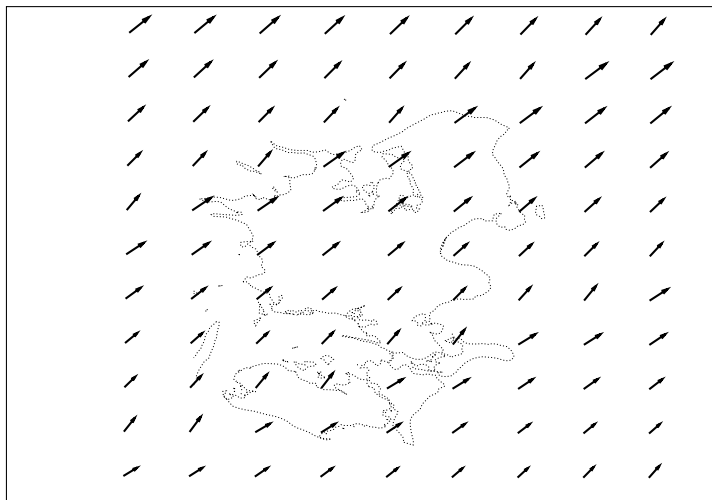


Figure 9: An example of the wind field from HIRLAM. A similar field is generated for Bornholm.

#### HIRLAM wind field

**Input to WASP** For WASP to be able to simulate the local effect input of the orography, roughness and obstacles is needed. In Figure 10 the orography and roughness of the

surroundings of the Kyndby wind farm are shown and in Figure 11 the obstacles of the Avedøre 1000 wind turbine are shown.

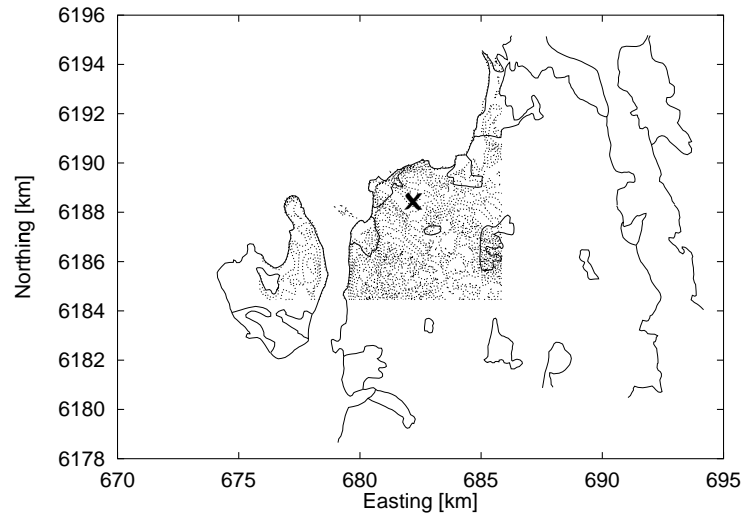


Figure 10: The orography (thin lines) and the roughness (thick lines) for Kyndby wind farm. This digital information is given as input to WSP. The cross marks the location of the wind farm.

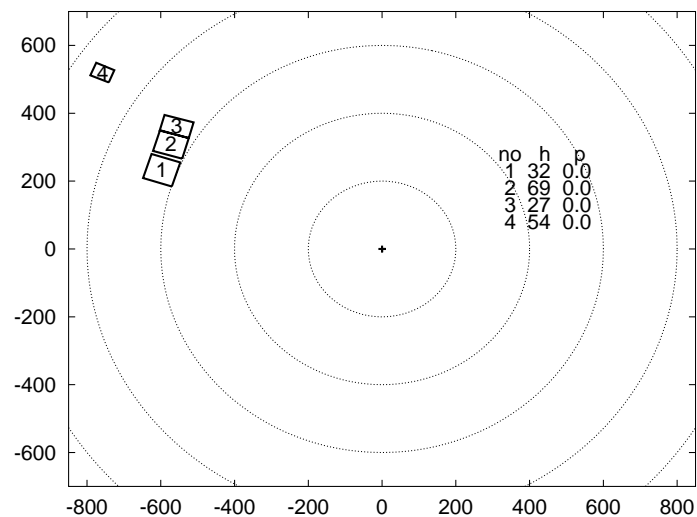


Figure 11: The obstacles input to WSP for the Avedøre 1000 turbine.

**Input to PARK** The PARK program needs as input the power and thrust curves (see Figure 12) and the wind farm lay-out (see Figure 13).

#### 4.4.8 Using the 10 m wind as input

Due to the decrease in grid size and the improvement of the boundary-layer parameterisation of HIRLAM, the level from which the wind has to be taken has changed from when the model was first developed and implemented (see [2] for further details). In the original model the wind found in model level 5 (approx. 550 m agl) should be used as the best approximation of the geostrophic wind, now, however, the wind from the lowest level has the smallest scatter when compared to the observed wind at the wind farm site.

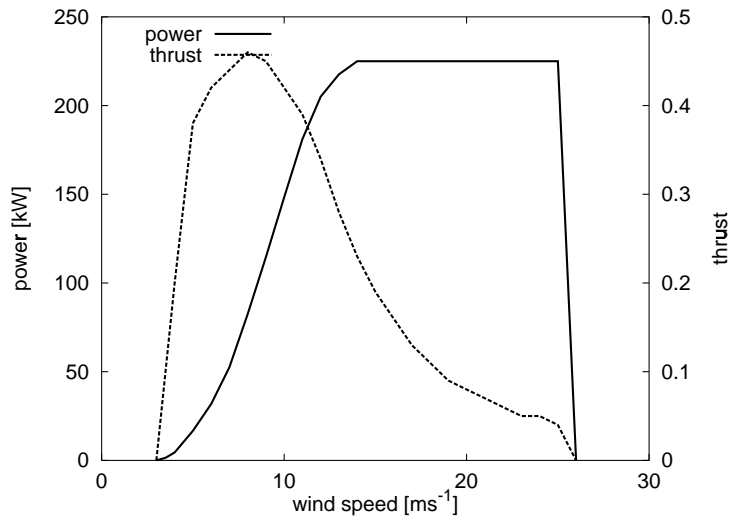


Figure 12: The power (solid line) and thrust curve (dashed line) of the Vestas V27 wind turbine.

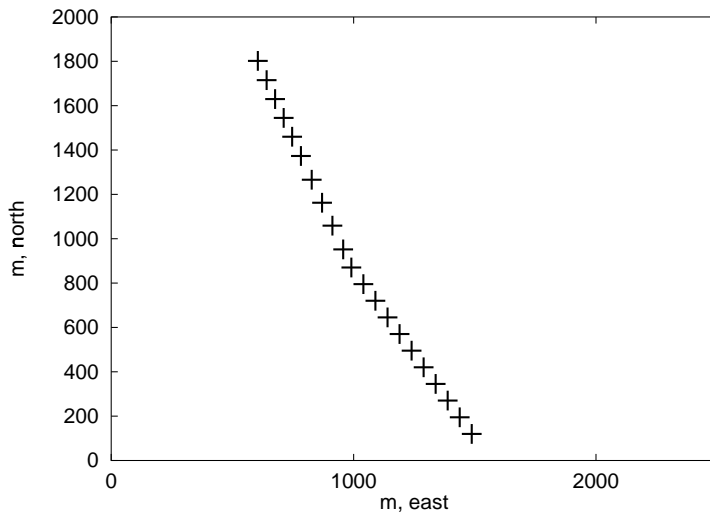


Figure 13: The lay-out of the Kyndby wind farm.

This means that since the original model had to transform the wind from a geostrophic wind via the geostrophic drag law to the surface the model must be changed, since this transformation has already been done by the HIRLAM model. Referring to Figure 2 the box labeled ‘Geo. drag law, Log profile’ must therefore be removed. Calculating the mean error and std. dev. of the original model and the model proposed here applied to the Risø mast, however, the predictions using the 10 m wind show a reduction in the standard deviation of typically 20% on the prediction of the wind speed.

## 4.5 Differences between Oldenburg and Risø Implementation

The main differences between the Risø and the Oldenburg online prediction model are

- Risø model is based on HIRLAM, Oldenburg model on the *Deutschlandmodell* NWP model, which has a higher spatial resolution.
- The Oldenburg approach is using a non-linear roughness model implementation.
- The Oldenburg model can handle wind farms with turbines of different hub heights.
- The Oldenburg model doesn't include obstacles.

# 5 Results and Conclusions

For the verification of prediction results, a lot of aspects have to be taken into account. In the beginning, the quality of the forecast will critically depend on the NWP model output itself. If this does not reflect the development of the weather situation, there is no chance to get a reliable local wind power prediction. The comparison of the influence of the two NWP models HIRLAM and *Deutschlandmodell* will be shown in section 5.7.

In general, the prediction quality depends on the prediction time. The prediction error is expected to increase for longer forecast horizons (chapter 5.3). But there are also other influences. The natural wind speed (in general) shows a daily pattern which can be reproduced more or less accurately by the wind speed prediction. We have a look at this effect in the “results” chapter where we mainly consider predictions with start time 00 UTC. So the results show the influence of the time of day. In general, the accuracy of a prediction for 36 hours may be different if the target time is 12 or 24 UTC (chapter 5.3).

*General remarks:*

- All predictions are based on the *Deutschlandmodell*, 0 UTC run, 10 m level, if nothing else is remarked.
- In general, the 1996 NWP grid data is used. If the basic year is 1997 (also grid data) or 1999 (online data), this is noted.
- In most cases, two basic statistical properties are used for discussion, the mean bias  $\langle(\text{predicted power} - \text{measured power})\rangle$  and the RMSE (Root Mean Square,  $\sqrt{\langle(\text{predicted power} - \text{measured power})^2\rangle}$ ).
- In many cases, the mean <sup>1</sup> value for all stations is used. This means that the RMSE are just summed up and divided by the number of stations. This of course is not equal to the RMSE of the summed up time series.

## 5.1 Wind Speed

First of all the quality of the wind speed prediction is evaluated. Figure 14 shows a scatter plot of the wind speed at 10 m level given by the *Deutschlandmodell* versus the measured wind speed at the same height for the station *Altenbeken*. The data for all prediction times is used to get enough data points. Generally, the prediction is systematically too low because most of the data points are below the bisector of angle. In particular, high wind speeds are underestimated. After the prediction of the NWP has been refined the predicted wind speed matches the measured wind speed much better. This can be seen in figure 15 where results of the refined prediction of the wind speed are compared to the measurements for the same station as before. The data points are now rather equally distributed along the bisector of angle. The improvement is mainly due to the detailed roughness description in the refinement which considers the local effects at the site in contrast to the direct *Deutschlandmodell* output which is based on a mean roughness over a large area.

---

<sup>1</sup>Sometimes we call this a *typical value*.

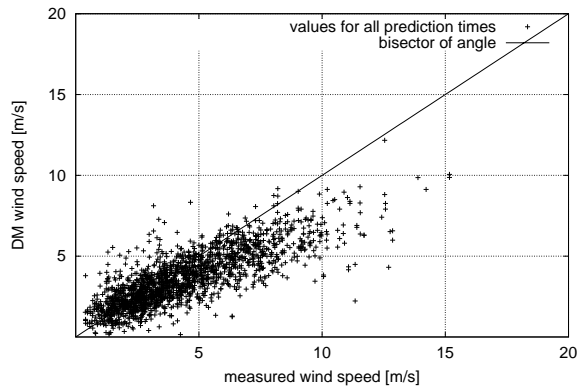


Figure 14: Scatter of measured and raw Deutschlandmodell wind speed at 10 m.

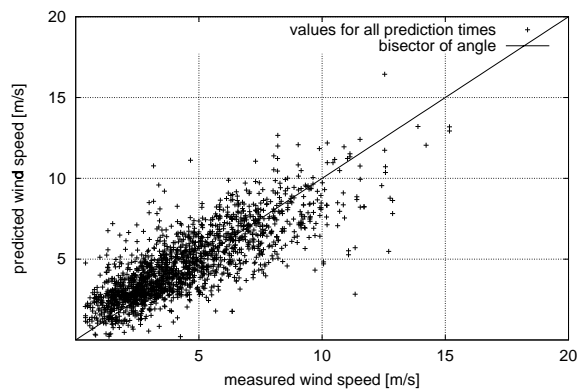


Figure 15: Scatter of measured and refined predicted wind speed at 10 m.

## 5.2 Power Prediction Time Series

In figure 16 a typical time series of measured and predicted power for a single turbine is shown. In general, the agreement is good and the two storm events are predicted quite well. Of course, the quality of the prediction is better for short forecast horizons, i.e. 6 h and 12 h. In figure 17 the predictions of three succeeding runs (0 UTC) are presented. Again the prediction is rather good but for large prediction times the forecast might deviate significantly from the real situation. This can be seen for the 24 h - 48 h forecast of run 1 which predicts small power output instead of a storm.

Figure 18 shows the RMSE between prediction (0 UTC run) and measurement of power outputs for different prediction times averaged over all sites. The upper curve is normalized to the respective mean power output. The RMSE value is very high (about 100%) and increases with prediction time, showing a daily pattern. The second (lower) curve shows the same RMSE normalized to the total rated power of all turbines regarded. This value, of course, is much lower. We will show later that this value is the more important one for a generalized proposition about the prediction uncertainty.

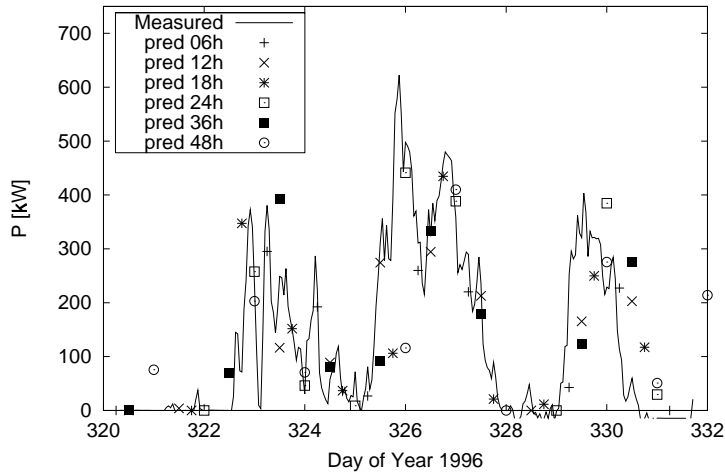


Figure 16: Typical time series of measured and predicted power for a single turbine in 1996.

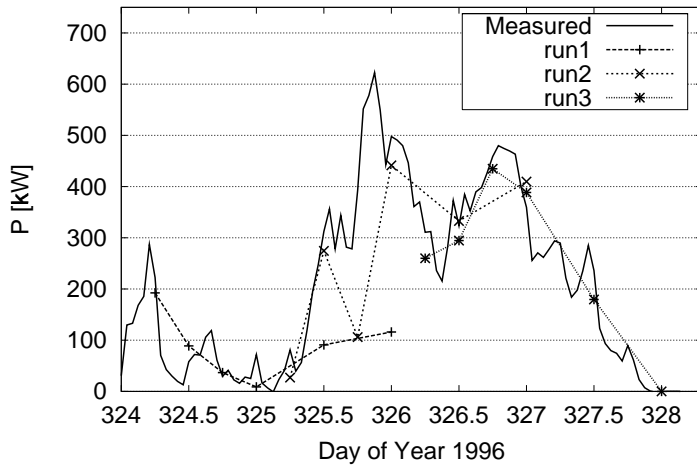


Figure 17: Detail of figure 16 showing development of three succeeding model runs.

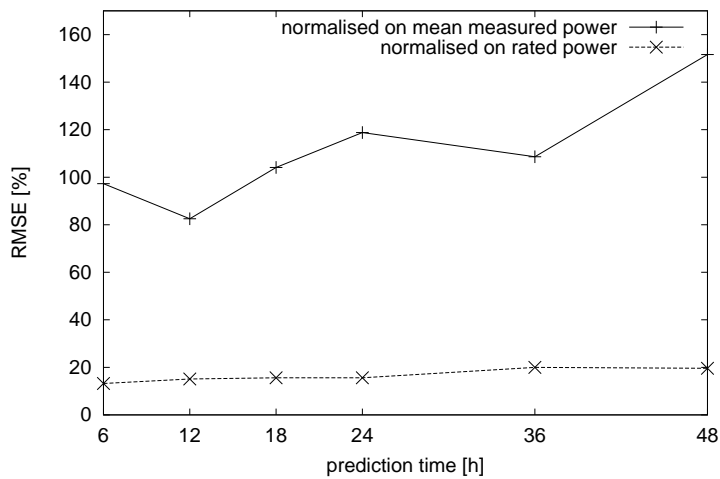


Figure 18: RMSE of power output versus prediction time, averaged over all stations. The upper curve is normalized to the current mean wind power, the lower one to the rated power of all turbines. The prediction error is increasing with prediction time.

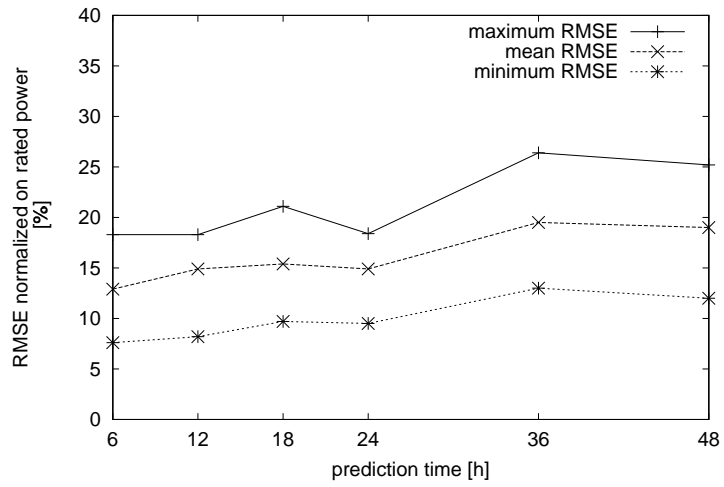


Figure 19: RMSE between prediction and measurement for all prediction times, mean over all stations and maximum and minimum value.

### 5.3 Prediction Horizon and Daily Pattern

Figure 20 shows the daily pattern of measurements and predictions (based on 10 m wind, 0 UTC run) for the cumulative power output of all stations. As expected, the wind speed is systematically higher at noon (12 and 36 hours prediction) than at night (24, 48 hours) due to the thermal stability state of the atmosphere. It can be stated in general that the relative daily pattern of the measurements is reproduced quite well, even if the absolute value of forecasts and measurements is quite different. This is true for sites with high as well as low daily variations (figures 21 and 25).

In figure 22 the development of the average of predictions is plotted for two different model levels (level 10 at 10 m mean height agl. and level 18 at 322 m). For the upper level the daily pattern of the forecast is just opposite to the expectations: the prediction at night is higher than at daytime. This holds for all levels from level 19 (133 m) and above. According to information provided by the DWD, this behaviour is an artifact due to an incomplete part of the model which implements the stability dependent momentum transfer in the lower boundary layer. In any case, it seems to be difficult to obtain a good forecast based on level 18 even after implementing a refinement including current stability of the atmosphere.

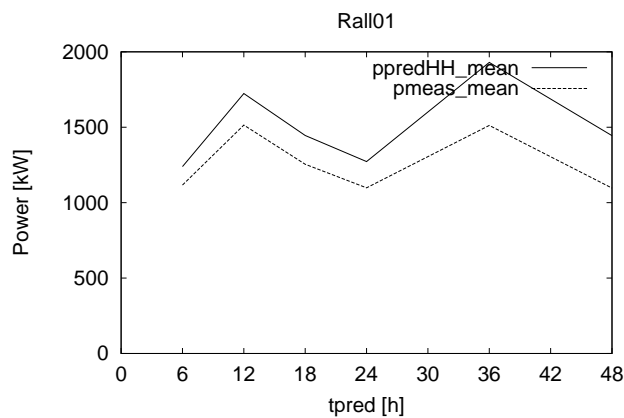


Figure 20: Daily pattern of measurements and predictions versus prediction time (here: = daytime). Sum of all stations. Both curves clearly show a daily pattern.

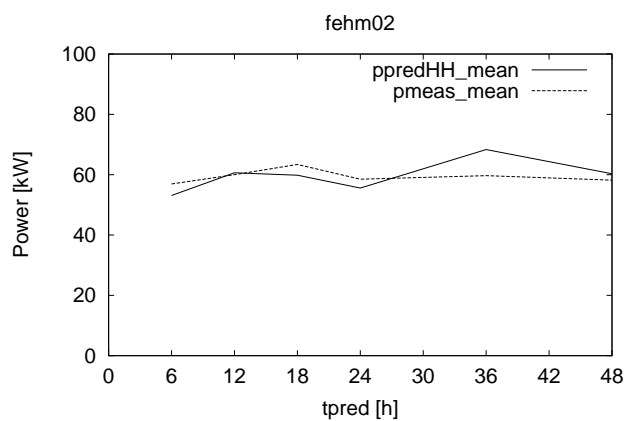


Figure 21: Example of daily pattern of the power prediction and measurement for a station with weak daily pattern (Fehmarn). This is also reproduced quite well by the predictions.

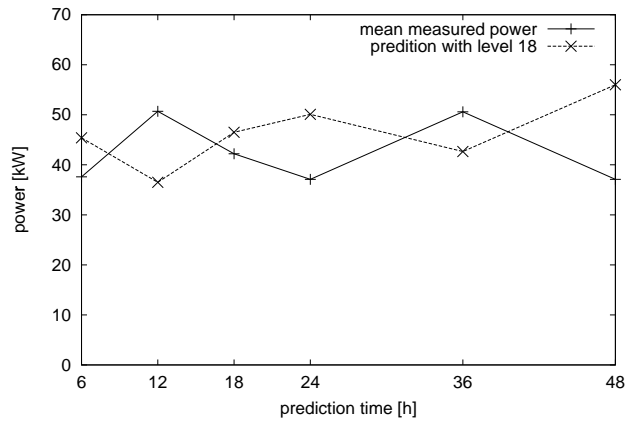


Figure 22: Daily pattern like in figure 20, level 10 (10 m height) and level 18 (322 m): The upper level shows a reverse daily pattern.

Figure 23 shows the behaviour of the predictions concerning the bias between power predictions and measurements depending on the prediction time for 1996 (annual means normalized to the measured mean). In any case, the prediction is higher than the measured output, and the mean value of the bias is increasing from 12 % at 6 hours to about 32 % at 48 hours. There seem to be mechanisms in the NWP model producing an increase of mean momentum with increasing prediction time.

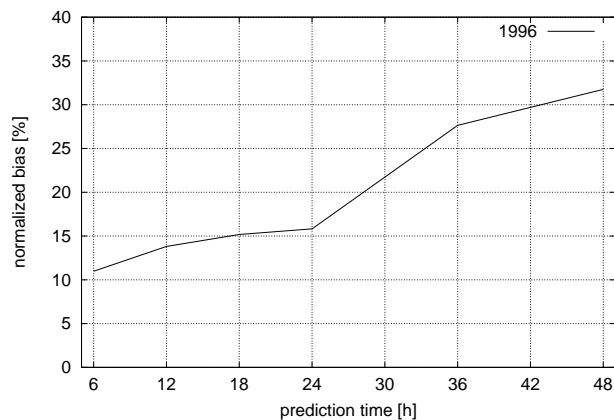


Figure 23: Prediction bias (predictions minus measurements) versus prediction time normalized to current mean power, mean of all stations. The bias is positive all the time and increasing with prediction time.

Figure 24 shows an example of the development of the RMSE for the station *Schülpl*. The values are normalized to the measured mean power and to the rated power, respectively, to get comparable statements. It can be seen that the RMSE normalized to the current mean power shows a distinct daily pattern while the one normalized to rated power does not. In fact, this behaviour shows a typical property of the prediction errors: the uncertainty of the prediction is mainly an absolute value which does not strongly depend on the current mean power output. This can be verified looking at the daily pattern of power output for the same site (figure 25): the development of the RMSE in figure 24 just reflects the normalization to the current mean power.

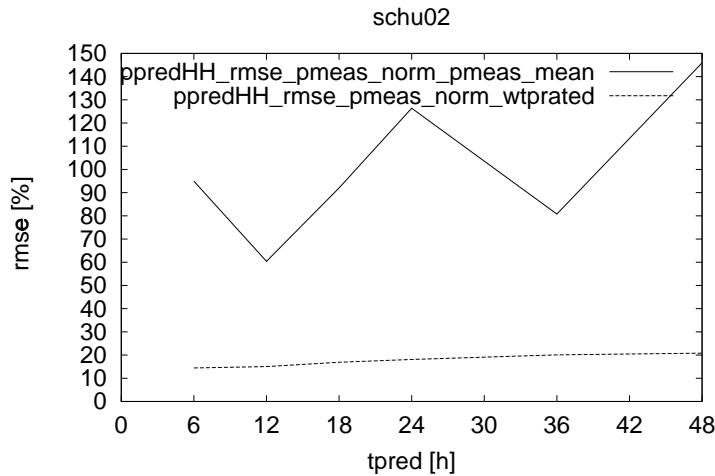


Figure 24: Example of RMSE versus prediction time for station Schülpl. The upper curve is normalized to the current mean wind power, the lower one to the rated power of the turbine. The prediction error is increasing with prediction time on average. It can be seen that the curve normalized to the rated power shows almost no daily variation, so the uncertainty of the prediction is mainly kind of an absolute error.

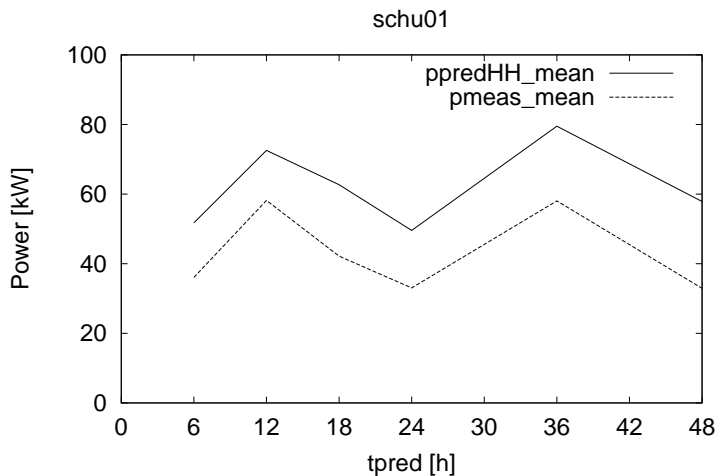


Figure 25: Daily pattern of measured and predicted power for station Schülpl.

The same behaviour can be seen for the mean RMSE over all stations shown in figure 26. On average the RMSE of a single station is rather high: about 100 % for 6 hours and about 150 % for 48 hours if normalized to the mean power output. If it is normalized to the mean rated power the RMSE ranges from about 17 % to 20 %. In contrast to this the RMSE of the summed power output of all turbines (figures 27 and 28) is much lower. Normalized to the mean power, the total RMSE increases from about 40 % (6 hours) to about 80 % (48 hours prediction). Normalized to rated power, the range of RMSE is increasing from about 7 % to 12 %. It must be noted that the fraction of annual mean to rated power is just about 15 % because there are some sites with quite poor wind conditions present in the ensemble of stations. The drastic improvement of the RMSE of the summed power output is due to the decay of the prediction error over a region. The greater the distance between the stations the less correlated their prediction error is. We will come back to regional effects in chapter 5.8.

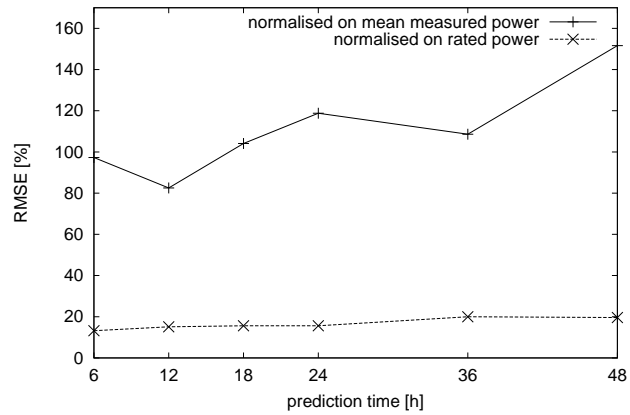


Figure 26: RMSE of power output versus prediction time, averaged over all stations. The upper curve is normalized to the current mean wind power, the lower one to the rated power of all turbines. The prediction error is increasing with prediction time.

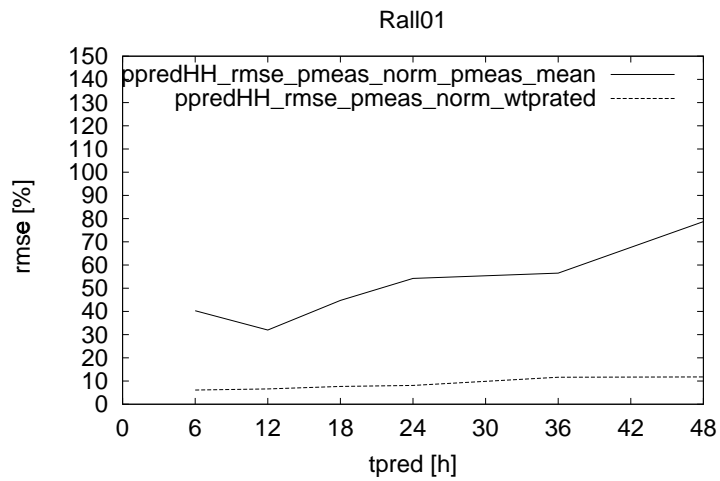


Figure 27: RMSE versus prediction time for sum of power output of all turbines. The upper curve is normalized to the current mean wind power, the lower one to the rated power of all turbines.

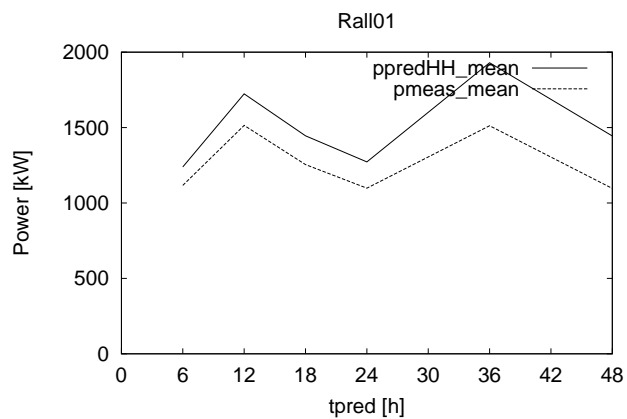


Figure 28: Mean power versus prediction time for sum of power output of all turbines, measured (dashed) and predicted (solid curve).

The increasing uncertainty of the forecast with increasing prediction horizon is also re-

flected in the correlation between prediction and measurements: for a typical site (figure 29), the correlation decreases from 0.88 (6 hours) to 0.72 (48 hours). For the summed up power output (figure 30), the figures are higher due to balancing effects (see chapter 5.8), but the overall development is the same (0.94 to 0.87).

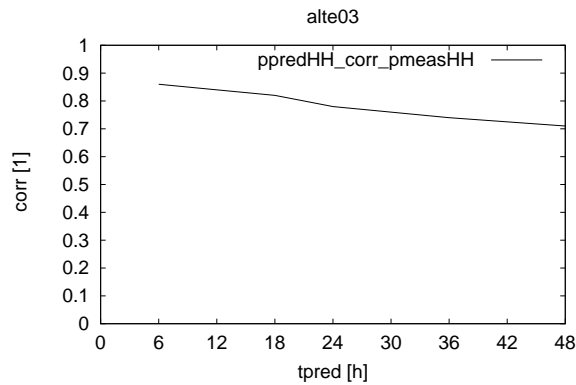


Figure 29: Example of correlation of the power prediction and measurement for the typical station Altenbeken. The correlation is decreasing with increasing prediction horizon. A slight influence of the time of day can also be seen.

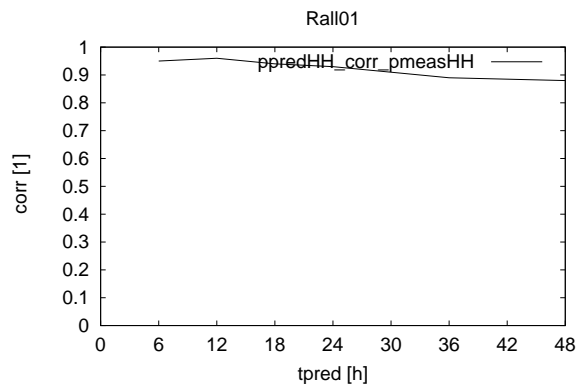


Figure 30: Correlation of prediction and measurement for summed power output of all stations. The correlation is quite high and decreasing with increasing prediction horizon. The influence of the time of day is very small.

## 5.4 Online Data 1999

For the year 1999 the data for our predictions is provided by online data from the DWD. In contrast to the 1996 grid data the 1999 online data is given directly for the geographic position of the station.

We found significant differences between the two years. Figure 31 shows a typical daily pattern of the mean predicted power output and the corresponding measurement. The prediction reveals a much more emphasized diurnal pattern as the measurement. Compared to 1996 the bias versus prediction times is completely different which can be seen in figure 32. The pronounced daily pattern can be seen there as well. Moreover, there is no systematic increase of the bias with increasing prediction time for 1999 which is the case for 1996.

The RMSE averaged over all station for 1999 does not increase with prediction time either (figure 33). The daily pattern is not much different from the one in 1996 shown in figure 26. The RMSE in 1999 is worse for short prediction times and better for large ones compared to 1996. It has to be noticed that the results for 1997 agree very well with 1996. The data source for these two years are grid points in contrast to online data in 1999. We have no information if the online data are subject to further post processing which might be responsible for the different results.

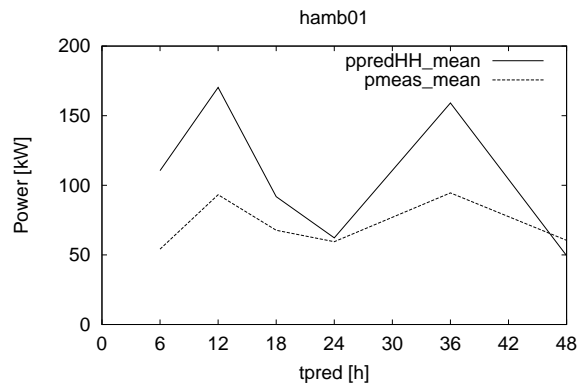


Figure 31: Daily pattern of measurements and prediction (1999). The daily variation of the forecast is too high.

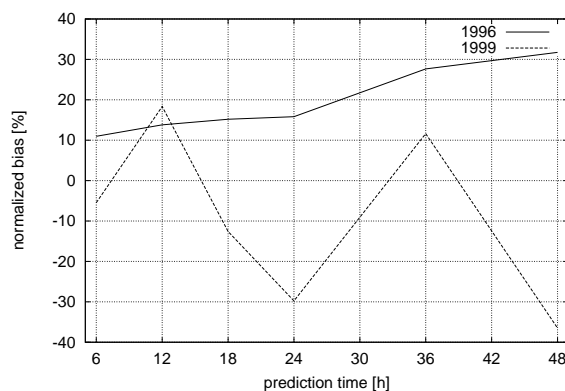


Figure 32: As figure 23, for 1999.

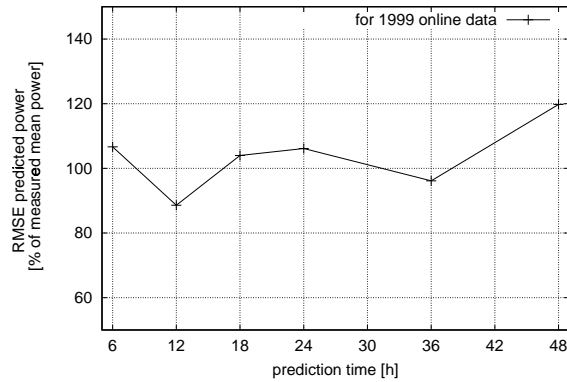


Figure 33: As figure 26, for 1999.

## 5.5 Prediction Error and Mean Power Output

In general, the quality of the prediction depends on the mean wind speed and power output respectively. As figure 35 shows, the relative RMSE of the forecast normalized to the current power output has almost the same value independent of the current mean power output except for low wind speeds. This is due to the fact that it is very difficult to predict low wind speeds correctly, because the lower atmosphere is not in equilibrium in many cases. In addition, the cut-in-performance of the turbine and the dependency of power output on  $u^3$  ( $u$ : current wind speed) causes big differences in power even for small wind speed differences.

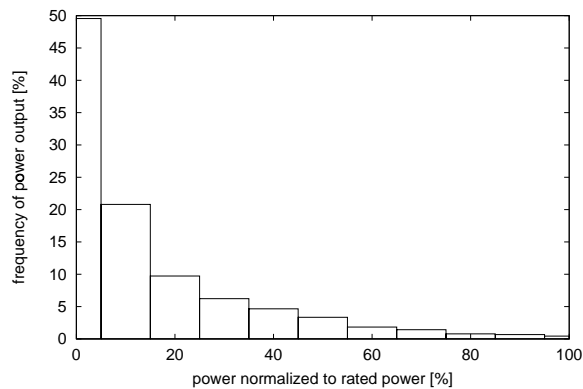


Figure 34: Distribution of power output for a typical site (Hilkenbrok)

Due to these reasons, the RMSE is dominated by the behaviour at low power outputs, because most time of the year, the wind speed itself is relatively low (figure 34). In reality, the prediction of power output is important mainly for higher wind speeds.

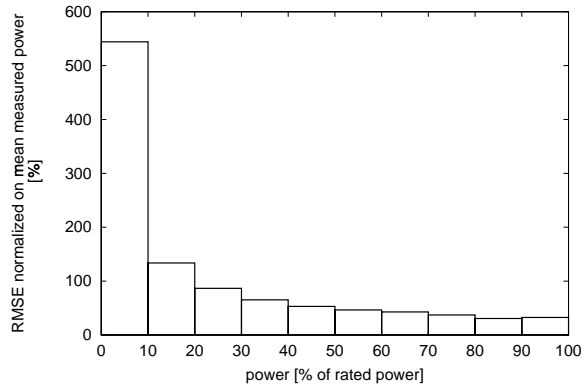


Figure 35: RMSE for classified for bins of mean measured power. The error for low wind speeds is very high.

From these facts, the idea arose to filter out low power outputs and just look at higher wind speeds. In general, this approach did not succeed due to several reasons:

- Filtering out low measured power outputs means also filtering out situations when the measured output is low and prediction is high. On the other hand, these are very bad situations because not having the expected wind power may be very expensive.
- This clear disadvantage cannot be overcome by filtering with respect to predicted power. In this case any change in the prediction model changes the value of the power output and in this way the ensemble of measurements regarded. This leads to totally incomparable results.
- Filtering may leave only a little number of observations left for bad sites. In this case, the statistical parameters calculated are very uncertain, and their absolute value (as e.g. the mean output after filtering) may be misleading.

As a conclusion, it can be stated that there is still a need to decrease the influence of low power outputs on statistical parameters, but a new algorithm has to be developed for this.

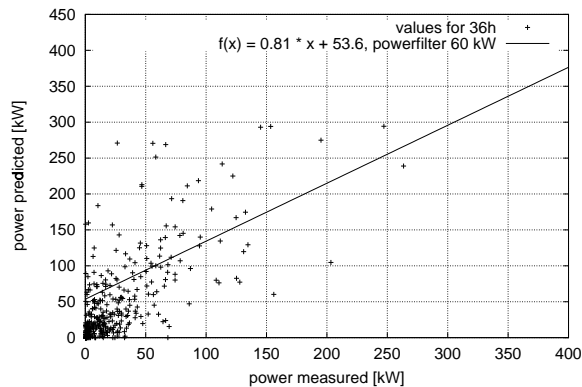


Figure 36: Scatter plot and regression line calculated with a power filter (regression with points were mean power is greater than 20 % of rated power = 60 kW) and for station Hagen-Dahl (36 hours prediction). The number of points left outside the filter rectangle (60 kW × 60 kW) is very small. The MOS regression line (here: offset and slope) is almost arbitrary.

## 5.6 MOS

The curve in figure 23 shows the mean bias for all sites between measurements and predictions. For all prediction times, the forecast is significantly higher than the measurements. This can be corrected partly by applying a simple MOS model, in this case by just multiplying the power forecast with a factor which is determined for each site averaged over all prediction times. Figure 37 shows an example for a site where this MOS can improve the predictions. Of course, there are sites where fundamental problems with the predictions for this site occur, e.g. station *Lindewitt*(figure 38). There prediction and measurements seem to be very weakly correlated. In a situation like that, an improvement by MOS would be just by chance.

In figure 39, the MOS factors gained from the 1996 data are plotted for each site, sorted by their magnitude. It can be seen that most values vary around an average of about 0.7 to 0.8, so this seems to be a quite universal value. Nevertheless there are some stations with values far away from that (e.g. 0.4).

Applying the MOS correction (factors from 1996) to the 1997 data leads to a bias shown in figure 40, lower curve. Generally, the prediction now underestimates the measurement but averaged over all prediction times the agreement between the predicted and measured mean power output has been improved by MOS.

The improvement in RMSE is shown in figure 41 and 42. Depending on the prediction time the RMSE normalized to the mean power output with MOS is between 10 % and 20 % smaller than without MOS. The RMSE with respect to the rated power is improved by about 2 %.

The results of the MOS correction for 1999 (factors from 1996) are given in figures 43 and 44. The bias has shifted on average by about -10 % compared to direct output (figure 32). Nevertheless, the RMSE has improved about 10 % for 6 and 12 hours. For larger prediction times (except 36 hours) the RMSE is worse with MOS than without (figure 33).

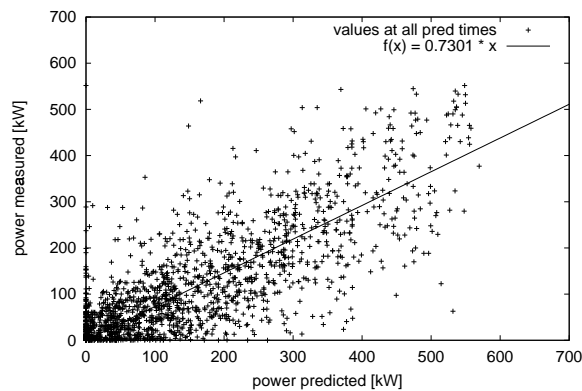


Figure 37: Scatter plot of measured versus predicted power with regression line for a “good” site (Wusterhusen). Simple MOS can improve the prediction significantly.

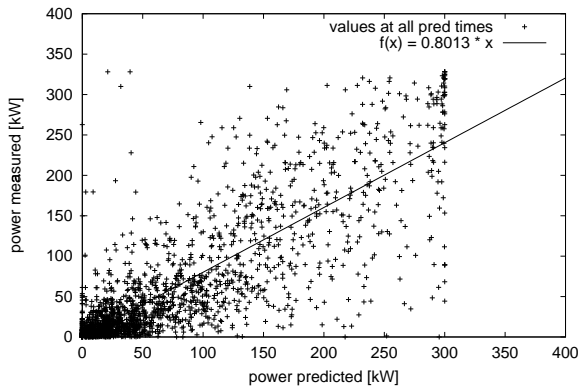


Figure 38: Scatter plot of measured versus predicted power with regression line for a “bad” site (Lindewitt). The scatter covers nearly the whole box inside rated power.

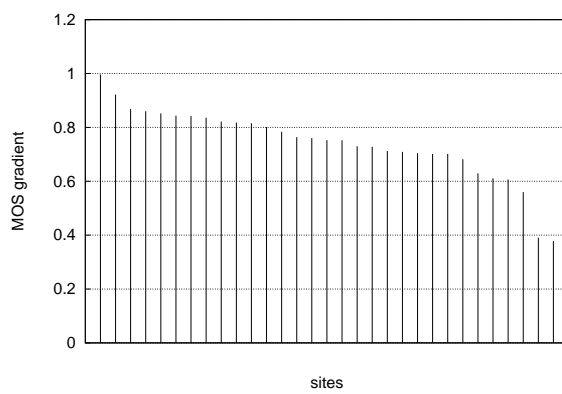


Figure 39: MOS factors for all sites.

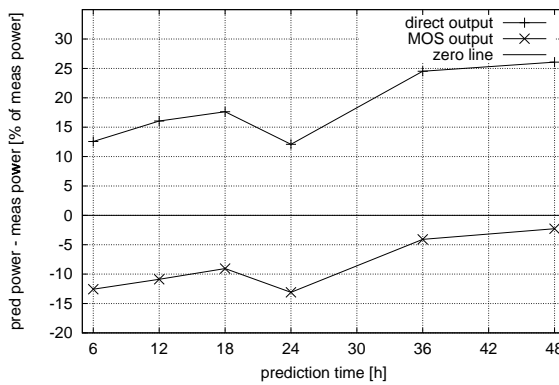


Figure 40: Bias between measurements and predictions with and without application of MOS versus prediction time normalized to measured power (1997 with MOS constants from 1996, average over all stations). The overall bias is decreased.

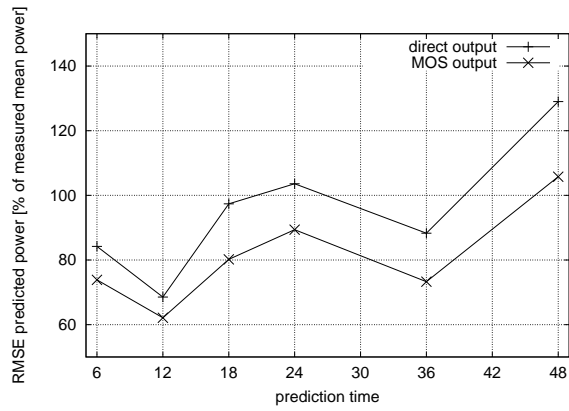


Figure 41: Like figure 40 for RMSE normalized to mean power.

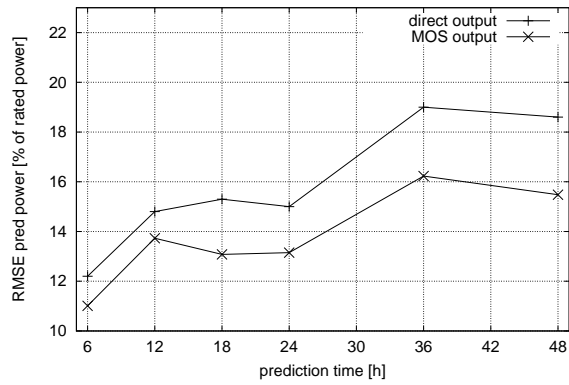


Figure 42: Like figure 40 for RMSE normalized to rated power.

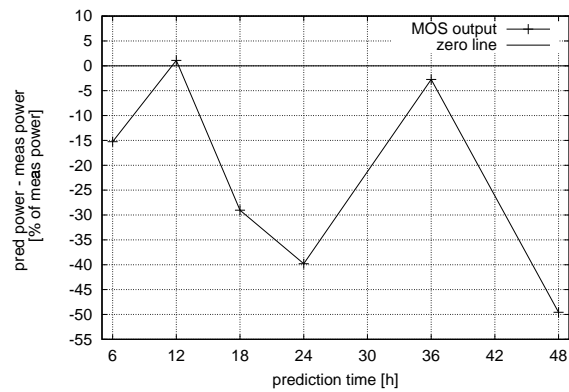


Figure 43: Like figure 40, bias for 1999 data.

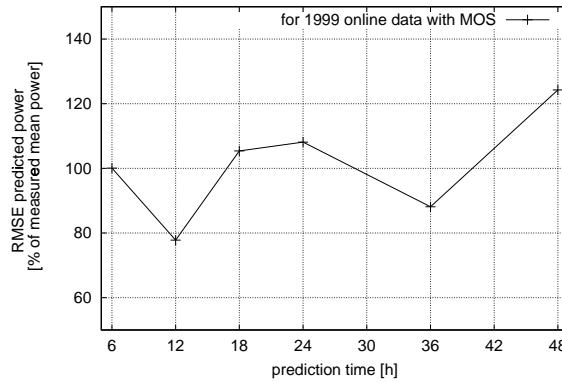


Figure 44: Like figure 40, RMSE for 1999 data.

## 5.7 HIRLAM/Deutschlandmodell

The forecast of the numerical weather prediction model is the basis of the whole forecast system. To compare two of the big models used in Europe, i.e. HIRLAM and *Deutschlandmodell*, seven sites are calculated with input data from both NWP models with the refinement implemented in Oldenburg (Oldenburg model) for 1999 prediction data (online data for both NWP models).

Figure 45 shows the bias between mean measured and mean predicted power for 1999 summed up over all 7 sites. HIRLAM overestimates for all prediction times nearly 10 kW in contrast to the *Deutschlandmodell* which generally fits quite good. The RMSE is more than 20% higher as can be seen in figure 46

Figure 47 shows the bias of measured and predicted power compared to the model implemented in Risø (Risø model) and the Oldenburg model. The Risø model overestimates for all prediction times with 15 kW. So the overestimation in figure 45 is not related to the refinement model, the origin lies in the NWP data already. Please note that both models were compared without MOS. It is expected that this would improve the performance if using HIRLAM input data distinctly.

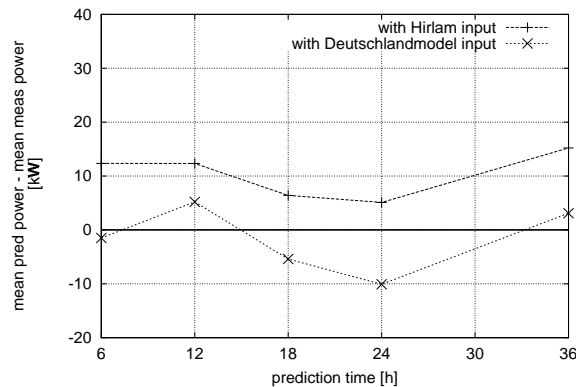


Figure 45: Bias between power output measurements and predictions with the Oldenburg model based on Deutschlandmodell and HIRLAM NWP data (1999).

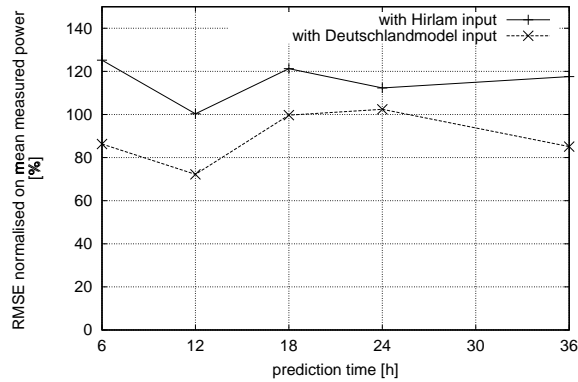


Figure 46: RMSE of power output measurements and predictions with the Oldenburg model based on Deutschlandmodell and HIRLAM NWP data, normalized to mean measured power(1999).

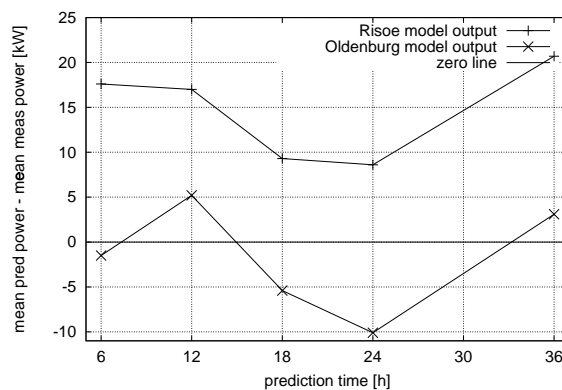


Figure 47: Bias between power output measurements and predictions of the Deutschlandmodell based Oldenburg and the HIRLAM based Risø model (1999).

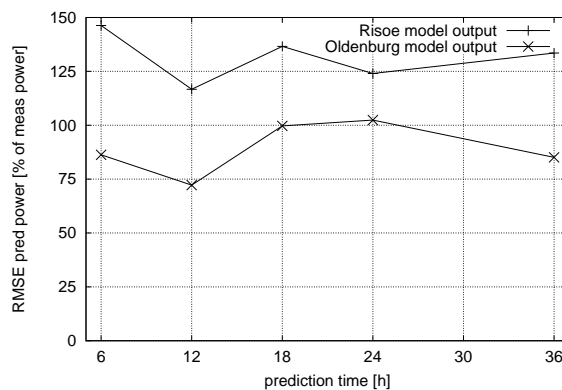


Figure 48: RMSE of power output measurements and predictions of the Deutschlandmodell based Oldenburg and the HIRLAM based Risø model (1999).

## 5.8 Prediction of the Power Output of Ensembles of spatially distributed Wind Wurbines

### 5.8.1 Relevance

For the implementation of prediction schemes into the scheduling processes of the conventional power plants, the key figure is not presented by the precision of the forecasted

power output of individual installations but of the power output of the ensemble of all turbines connected to the respective grid section. Thus, the error in the forecasted total power output has to be analysed. This is done by both the direct comparison of the lumped figures of measured and predicted power output of different ensembles and the in depth study of the correlation characteristics of the spatial field of forecast errors. From the latter tools for the assessment of forecast errors for arbitrary wind turbine ensembles may be derived. In the next section first the underlying fundamentals for the handling of statistical characteristics of ensemble effects are presented.

## 5.9 Ensemble Smoothing of Forecast Errors

Based on the complete set of the data for 33 turbines, the normalized prediction error (measured as rms error) for the ensemble power output is derived for the different forecast horizons. The results using the outcome of the full prediction model are presented in figure 49. The plot gives the average of the normalized forecast errors for the individual turbines and the ensemble figures.

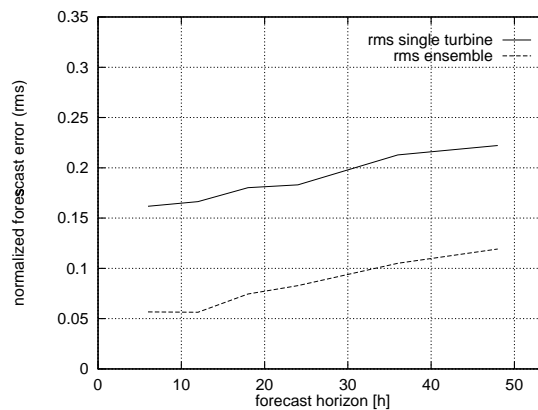


Figure 49: Normalized rms errors for the prediction of the power output of single turbines and the ensemble of 33 turbines.

The ratio of the forecast errors for the ensemble and single site data ranges from 0.38 for the time horizon 6h to 0.55 for 48 h. Compared to the value of 0.17 expected for this ratio assuming 33 uncorrelated data sets, this indicates, that the forecast errors show some coherence for the area inspected. This effect is more prominent with increasing forecast horizon.

### 5.9.1 Cross-correlation structure of the forecast errors

In this section the cross correlation of the forecast errors are inspected with respect to inter site distance, forecast horizon, sub-region and forecast model. First a total data set for 33 turbines is analysed. For the different forecast horizons the cross-correlation value for each pair of turbines is calculated using all available data for one year. For the presentation of results, the data are grouped according to inter site distance applying a class width of 25 km. Within each distance class, the average cross-correlation value for the pairs within the class is calculated. Figure 50 shows the outcome for the forecast horizons of 6, 12, 24 and 48 h.

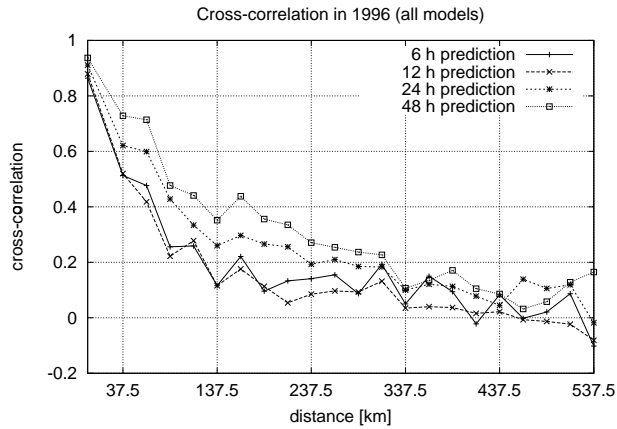


Figure 50: Cross-correlation of the forecast errors of the power output of pairs of sites using the complete ensemble. Presented are the averages of the cross-correlation for distance classes with a width of 25 km. The lines refer the forecast horizons of 6, 12, 24 and 48 h.

A first view shows, that the correlation decreases with inter site distance ranging from about 0.9 for turbine pairs within one wind farm to values around zero for the largest values of the inter site distance. Regarding the different forecast horizons the tendency that the correlation increases for longer horizons may be seen. For the 6 and the 12h forecast however, the correlation data are almost identical. The increase of the correlation with the forecast horizon is in accordance with the ratios of the ensemble smoothing for the forecast errors presented in section 5.10 and 5.10.1.

Summing up the following statements can be made:

- The cross-correlation of the forecast error decreases with inter station distance. For distances above about 300 km the cross-correlation approaches zero for all forecast horizons.
- In general, the cross-correlation increases with increasing forecast horizon. For the 6h and 12h horizon the differences in correlation are only marginal.
- The correlation structure of the forecast error is not significantly effected by various stages of included details of the forecast model. ? There are no significant differences in the correlation characteristics within the inspected sub ensembles.

## 5.10 Different Regions

For a quantitative look at the smoothing effects of the geographical dispersion of the turbines, the existing measuring sites were summed up to regions with three typical maximum distances: 140 km (figure 51), 350 km (figure 52) and all sites (700 km). Then the RMSE of measurements and predictions were calculated and normalized to the average RMSE of a single turbine. As comparison, the maximum expected reduction ( $\frac{1}{\sqrt{N}}$ , N: number of turbines in a region, see above) is given also. As expected, for longer prediction times the reduction of error is smaller due to systematic, correlated errors of the predictions. In all cases, the reduction is small for the 12 and 36 hours prediction, which points to a systematically insufficient prediction of the daily wind speed pattern (input for the calculation were the 00 UTC prediction run).

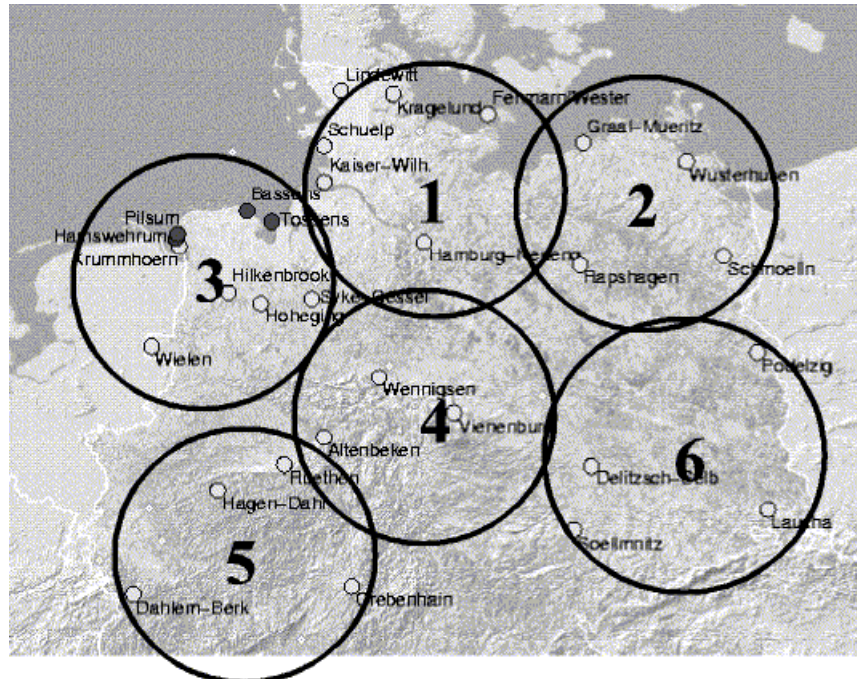


Figure 51: Definition of regions with typical radius of 140 km.

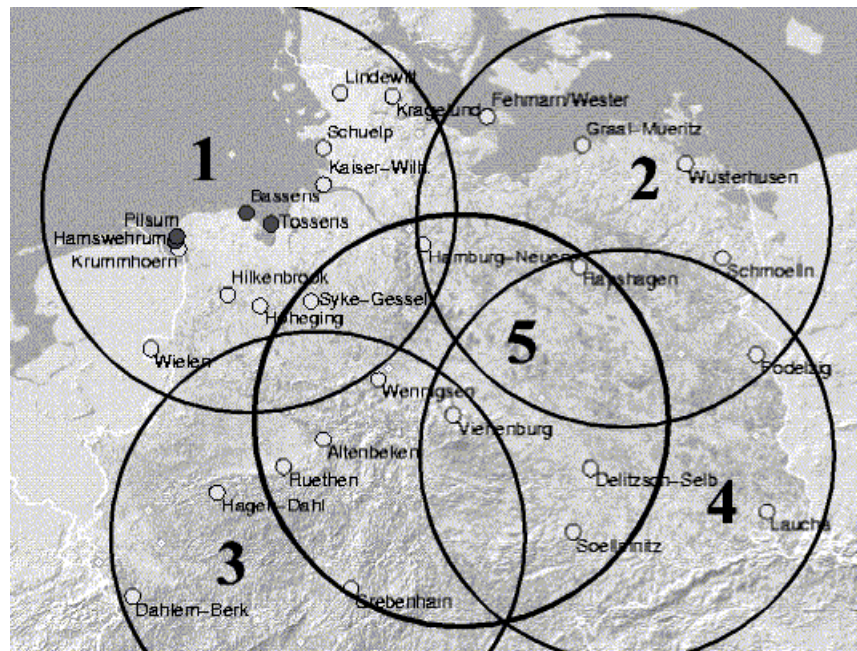


Figure 52: Definition of regions with typical radius of 350 km.

Prediction time		6	12	18	24	36	48
Region size	$(\sqrt{N})^{-1}$						
140 km	0.71	0.81	0.95	0.87	0.82	0.99	0.82
350 km	0.45	0.63	0.66	0.68	0.64	0.73	0.66
700 km	0.17	0.41	0.41	0.42	0.45	0.53	0.51

Table 2. Ratio of RMSE for different regions and mean RMSE for single sites.  $N$  is the number of sites within the region.

### 5.10.1 Application for Model Regions

To get an impression of the prediction improvement, model calculations were made with the correlation of prediction errors depending on distance as input. Two model regions were defined,  $45 \times 150 \text{ km}$  and  $225 \times 150 \text{ km}$ , corresponding to typical sizes of energy supply areas in Germany. The grid spacing was chosen as the resolution of the *Deutschlandmodell* model ( $15 \text{ km}^2$ ). All correlations of turbines with a smaller mutual distance were set to 1. For the calculations, the correlations were fitted by the function  $r(\Delta T) = 1 - \exp(-a * R)$  with  $r$ : correlation,  $\Delta T$ : prediction time,  $R$ : distance between sites, and  $a$ : constant to be determined.

In table 3 the reduction factors of the prediction errors are listed. It shows that the error is reduced to 83 % for the small and to 74 % for the larger area compared to the typical error for a single site.

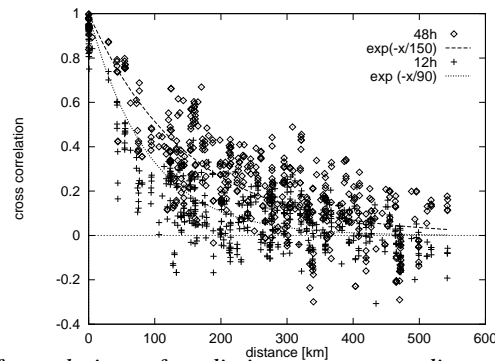


Figure 53: Fit of correlations of prediction error versus distance as in figure 50.

Time Horizon	Area $45 \times 150 \text{ km}$	Area $225 \times 150 \text{ km}$
12 h	0.76	0.62
48 h	0.83	0.74

Table 3. Ratio of regional by average single site standard deviation for two typical regions. Grid spacing of the NWP is 15 km.

## 5.11 Conclusions

- In general it can be stated that the development of wind farm production is predicted quite well by the forecasting system. Nevertheless there are situations where bigger deviations between forecast and actual power output occur.
- The daily pattern of wind power output is reproduced well by the NWP grid data. The online data overestimates the diurnal amplitude. It is possible that at the weather service an internal MOS model is applied to the online data already which leads to this different behaviour.
- The deviations between measured and predicted power outputs assessed in terms of RMSE are quite high and in the order of magnitude of the mean power output. On the other hand, the RMSE error is almost independent of the current mean power output (except for very low wind speeds). This means that the prediction error is kind of an absolute measure, which is typically in the range of 15 % (6 hours prediction) to 25 % (48 hours) of rated power.
- The predictions for all models show a bias compared to measurements. An MOS procedure must be included into the prediction system in any case. The MOS parameters are depending on the current prediction model version and must be adapted

from time to time. The decrease of RMSE by MOS is typically about 15 % of its original value.

- The comparison of the two NWP models, *Deutschlandmodell* and HIRLAM has shown a better performance for the German model. This may be due to a higher bias shown by the HIRLAM forecasts which could be decreased by MOS. This feature should be analysed on a larger data set of prediction and measurement data.
- For the current status of the forecast model, assessments of the forecast errors for the output of wind turbine ensembles may be based on the information of the inter site distances and the forecast horizon involved. For larger distances, prediction errors between different sites are just partly correlated.
- For regions with a size typical for the supply area of a utility, the single site forecast error may be reduced by a factor of 0.60 to 0.85, depending on the prediction time and actual size of the region.

## 6 Exploitation

From the output of this project, Risø and Oldenburg hold a wind power prediction model. The main differences are the different NWP input (Danish HIRLAM and German DM) and a slightly different refinement procedure. Each of the models includes the improvements gained through this project and both models are operational. Each institution is holding the property rights to their own model.

In Germany, the main goal of exploiting the output of this project is to install the prediction system for Germany on a commercial bases, most likely together with the *German Weather Service* DWD. To do this, the system must be endorsed by a data base including the characteristic data of wind turbines installed in Germany. This database is under development already.

In Denmark, the Risø model is in a mature state of commercialisation: sold to one utility already (which was not a project partner) and under negotiation with another two. There are also approaches to install this system at other European countries.

# Acknowledgements

The project has been funded by the Commission of the European Communities under the JOULE programme, contract JOR3-CT98-0272. The development of the Risø model was as funded by the EFP-programme under the Danish Ministry of Energy and the Environment, contract 1363/94-0005 and JOULE contracts JOUR-0091-MB(C) and JOR3-CT95-0008.

# 7 Characteristic Diagram

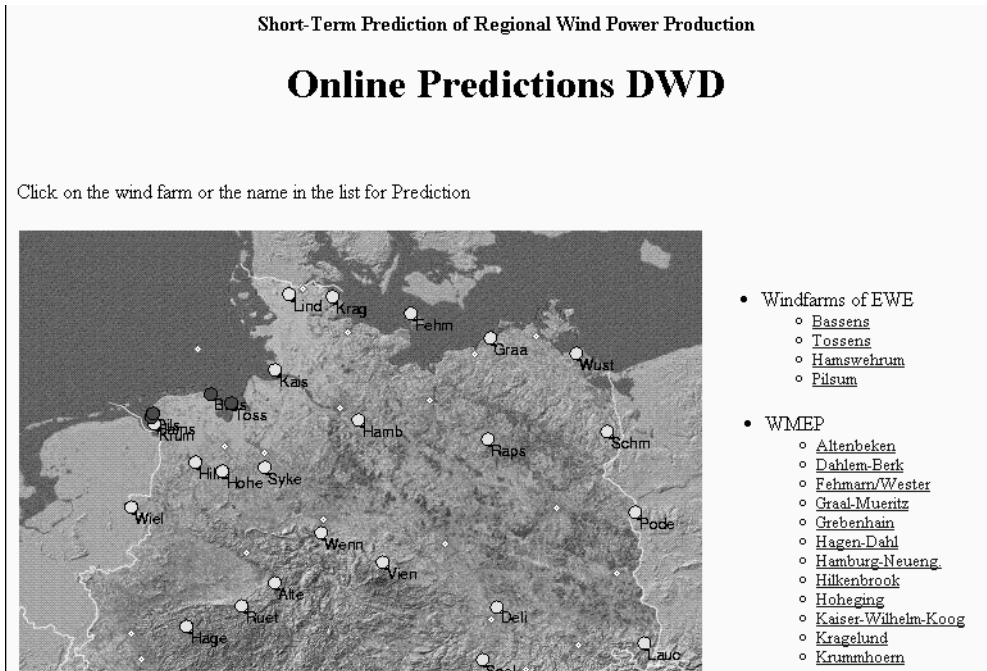


Figure 54: Access HTML page to the wind power prediction system. The clickable map shows the sites for which predictions are available.

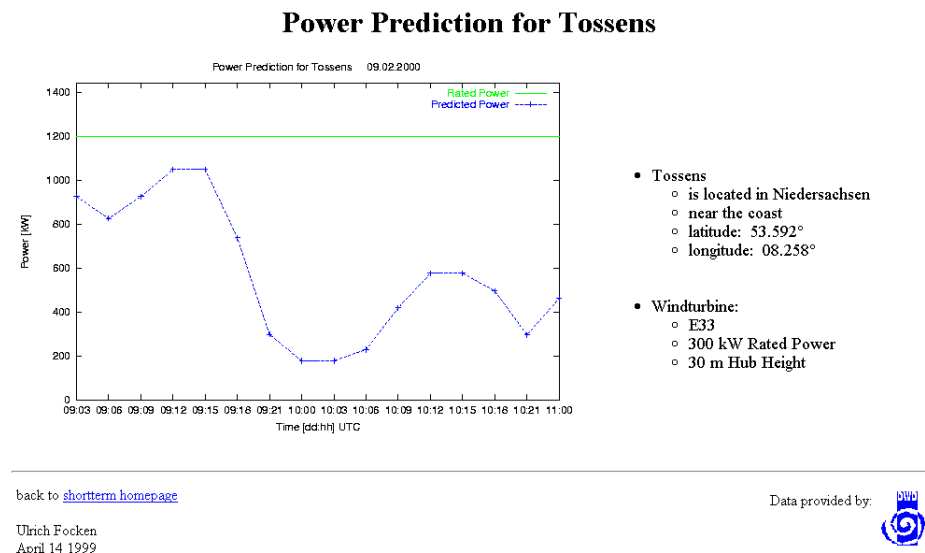


Figure 55: Chart of wind power predictions for one site. The predicted development of the wind power for two days ahead is shown.

# A References

## References

- [1] L. Landberg, S. J. Watson, J. Halliday, J. U. Jørgensen and A. Hilden, 1994: *Short-term prediction of local wind conditions*, Risø-R-702(EN), Risø National Laboratory, Roskilde, Denmark.
- [2] Joensen, A, G Giebel, L Landberg, H Madsen, 1999: *Model Output Statistics Applied to Wind Power Prediction*. Proceedings from EWEC99, Nice (FR).
- [3] Landberg, L and A Joensen, 1998: *A model to predict the power output from wind farms - an update*. In proceedings from BWEA 20, Cardiff(UK), 127–132.
- [4] Landberg L. and S.J. Watson, 1994: *Short-term prediction of local wind conditions*. To appear in *Boundary-Layer Meteorology*.
- [5] L. Landberg and M. A. Hansen and K. Vesterager and W. Bergstrøm, 1997: *Implementing Wind Forecasting at a Utility*, Risø-R-929(EN), Risø National Laboratory, Roskilde, Denmark.
- [6] Machenhauer, B. (ed), 1988: *HIRLAM final report*. HIRLAM Technical Report 5, Copenhagen, Denmark.
- [7] Mortensen, N.G., L. Landberg, I. Troen and E.L. Petersen, 1993: *Wind Atlas Analysis and Application Program (WASP), User's Guide*. Risø-I-666(EN)(v.2), Risø National Laboratory, Roskilde, Denmark. 133 pp.
- [8] Mortensen, N.G., D.N. Heathfield, L. Landberg, O. Rathmann, I. Troen and E.L. Petersen, 2000: *Wind Atlas Analysis and Application Program: WASP 7.0 Help Facility*. Risø National Laboratory, Roskilde, Denmark. 277 pp. ISBN 87-550-2667-2.
- [9] Sanderhoff, P, 1993: *PARK – User's Guide. A PC-program for calculation of wind turbine park performance*. Risø-I-668(EN), Risø National Laboratory, Roskilde, Denmark. 8 pp.
- [10] Troen and Petersen, 1989: *The European Wind Atlas*. Published for the CEC by Risø National Laboratory, Roskilde, Denmark. 656 pp.
- [11] Landberg L, S J Watson, J A Halliday, J U Jørgensen and A Hilden, (1994), *Short Term Prediction of Local Wind Conditions*. Final report to EC for contract JOUR-0091-C(MB).
- [12] Watson S J, L Landberg and J A Halliday, (1994), *IEE Proc. C* **141**, pp 357–362.
- [13] Roland B. Stull, (1988), *Introduction to Boundary Layer Meteorology*. Published by Kluwer Academic Press.
- [14] Anna M. Sempreviva, (1990), *Response of Neutral Boundary Layers to Changes of Roughness*. *Boundary-Layer Meteorology*, 1990, no. 50.
- [15] P.S. Jackson and J.C.R. Hunt, (1975), *Turbulent wind flow over a low hill*. *Quarterly Journal of the Royal Meteorological Society*.
- [16] Majewski D., R. Schrodin et al.: *Dokumentation des EM/DM-Systems*. Deutscher Wetterdienst, Abteilung Forschung, internal report. 1995.
- [17] I. Katic: *Program Park, Calculation of Wind Turbine Park Performance*. Technical report Risø National Laboratory, Risø 1989.
- [18] [http://reisi.iset.uni-kassel.de/wind/reisi\\_dw.html](http://reisi.iset.uni-kassel.de/wind/reisi_dw.html)

## B List of publications

This chapter contains a list of all the publications written by the partners in connection with the project and similar EU-funded projects .

### Risø

- Landberg, L, 1996: Implementing prediction of power from wind farms at utilities. In proceedings from EUWEC 96, Göteborg, 592-595.
- Landberg, L, 1996: Implementing prediction of power from wind farms at utilities. In proceedings from BWEA 18, Exeter, 271–276.
- Landberg, L, 1997: A model to predict the power output from wind farms. In proceedings from Windpower '97, Austin, 443-451.
- Landberg, L, 1997: A mathematical look at a physical power prediction model. In proceedings from Windpower '97, Austin, 629-636.
- Landberg, L, 1997: Short-term prediction of wind farm power output - from theory to practice. In proceedings from BWEA 19, Edinburgh(UK), 16-18 July, ed. R Hunter, 397-402.
- Landberg, L, 1998: Predicting the power output from wind farms. In proceedings from EWEC '97, Dublin, 747-750.
- Landberg, L, 1998: A mathematical look at a physical power prediction model. In proceedings from EWEC '97, Dublin, 406-408.
- Landberg, L, 1997: Program spår om vinden (in Danish, Program predicts the wind). *Vedvarende Energi & Miljø*, 6, 8-9.
- Landberg, L and A Joensen, 1998: A model to predict the power output from wind farms - an update. In proceedings from BWEA 20, Cardiff(UK), 127-132.
- Landberg, L, 1999: Short-term prediction of the power production from wind farms. *J. Wind Eng. Ind. Aerodyn.*, 80, 207-220.

### Oldenburg and Magdeburg (partly)

- H.G. Beyer, D. Heinemann, H. Mellinshoff, K. Mönnich, H.-P. Waldl, 1998: Vorhersage der regionalen Leistungsabgabe von Windkraftanlagen. Tagungsband der 4. deutschen Windenergiekonferenz 1998, Wilhelmshaven.
- H.G. Beyer, H. Mellinshoff, K. Mönnich, H.-P. Waldl, 1998: Anwendung von Windvorhersagen des Deutschen Wetterdienstes zur Windleistungsprognose im Zeitbereich 6 – 24 h: eine exemplarische Untersuchung für Standorte in Mecklenburg-Vorpommern. Tagungsband der 4. deutschen Windenergiekonferenz 1998, Wilhelmshaven.
- H. Mellinshoff, 1998: Entwicklung und Verifikation eines Modells zur Vorhersage der Leistungsabgabe von Windkraftanlagen auf der Basis numerischer Wettervorhersagen. Masters Thesis, 1998, Carl von Ossietzky Universität Oldenburg.
- H.G. Beyer, H. Mellinshoff, K. Mönnich, H.-P. Waldl, 1998: “Und nun zum Wetter . . . ”: Windleistungsvorhersage. *Erneuerbare Energien*, June 1998, pages 33 – 35.
- H.G. Beyer, H. Mellinshoff, K. Mönnich, H.-P. Waldl, 1998: Windleistungsvorhersage im Zeitbereich bis 48 Stunden. *DEWI-Magazin*, August 1998, number 13, 49 – 53.

- H.G. Beyer, H. Mellinghoff, K. Mönnich, H.-P. Waldl, 1998: Adaption meteorologischer Methoden für die Vorhersage der Leistungsabgabe von Windkraftanlagen für die Kraftwerkseinsatzplanung. Spring conference of the DPG (german physical society), 1998.
- H.G. Beyer, H. Mellinghoff, K. Mönnich, H.-P. Waldl, 1998: Vorhersage der Leistungsabgabe von Windkraftanlagen zur Einsatzplanung konventioneller Kraftwerke. Kongreß Erneuerbare Energie '98, Hannover Trade fair, April 1998.
- H.-P. Waldl, 1998: Und nun zum Wetter . . . Windenergieforschung in Oldenburg. Day of Physics, University of Oldenburg, 1998.
- H.-P. Waldl, 1998: Beitrag der Windenergienutzung zur Stromversorgung und zum Klimaschutz, Pressekonferenz Bonn BWE, September 1998.
- H.-P. Waldl, 1998: Windleistungsprognose bis 48 Stunden. Initiative Zukunftsennergien NRW, December 1998.
- H.-P. Waldl, 1999: Aktuelle Themen der Windenergiemeteorologie – Windleistungsprognose und Anwendung mesoskaliger Strömungsmodelle. Physikalisches Kolloquium, Carl von Ossietzky Universität Oldenburg, April 1999.
- H.G. Beyer, D. Heinemann, H. Mellinghoff, K. Mönnich, H.P. Waldl, 1999: Forecast of regional power output of wind turbines. Proceedings of the European Wind Energy Association Conference and Exhibition, Nice, France, 1999, pages 1070-1073.
- G. Giebel, L. Landberg, K. Mönnich, H.P. Waldl, 1999: Relative Performance of different numerical weather prediction models for short term prediction of wind energy. Proceedings of the European Wind Energy Association Conference and Exhibition, Nice, France, 1999, pages 1078-1081.
- Hans-Peter Waldl, Kai Mönnich, 1999: Dem Wind auf der Spur. Neue Energie, May 1999, pages 46 – 48.
- Kai Mönnich, 2000: Vorhersage der Leistungsabgabe netzeinspeisender Windkraftanlagen zur Unterstützung der Kraftwerkseinsatzplanung. PhD-Thesis, Carl von Ossietzky Universität Oldenburg, 2000, in preparation.
- U. Focken, M. Lange, K. Mönnich, H.-P. Waldl, H.G. Beyer, A. Luig, 2000: Regionale Unterschiede und räumliche Ausgleichseffekte bei der Vorhersage der Leistungsabgabe von Windkraftanlagen. Deutsche Windenergiekonferenz, Wilhelmshaven, June 2000, submitted.
- G. Giebel, H.-P. Waldl, 2000: Einfluß des dänischen und des deutschen Wettervorhersagemodells auf die Qualität einer 48 h-Windleistungsprognose. Deutsche Windenergiekonferenz, Wilhelmshaven, June 2000, submitted.